CYTOPLASMIC ADAPTOR PROTEIN MIG-10 INTERACTS WITH ABELSON TARGET ABI-1 DURING NEURONAL MIGRATION IN *C. ELEGANS*

A Thesis

Submitted to the Faculty of Worcester Polytechnic Institute

In partial fulfillment of the requirements for the Degree of Master of Science

By Erin K Flaherty

Approved:

_____	_____	_____
Elizabeth Ryder, PhD	Joseph Duffy, PhD	Jagan Srinivasan, PhD
Major Advisor	Committee Member	Committee Member
WPI	WPI	WPI

Contents

Table of Contents

Abstract

Cellular migration is an essential process for establishing neural connections during development. The MIG-10/RIAM/Lamellipodin signaling proteins are thought to send positional information from guidance cues to actin polymerization machinery, promoting the polarized outgrowth of axons. In *C. elegans*, mutations in the gene *mig-10* result in the truncation of the migration of the mechanosensory neurons. Biochemical analysis demonstrates that MIG-10 interacts with abelson-interactor protein 1 (ABI-1), and therefore investigation into whether these proteins work together in the neuron to promote migration was completed.

To demonstrate MIG-10 cell autonomy in the neuron, transgenic strains with specific expression of *mig-10* were created. *mig-10* mutants were rescued in the mechanosensory, anterior lateral microtubule neuron (ALM) by neuron specific expression of *mig-10* but not by epithelial expression, suggesting that MIG-10 is acting cell autonomously. To determine ABI-1 cell autonomy, transgenic strains with specific neuronal expression of *abi-1* were compared to the wild type strain. *abi-1* mutants were rescued by neuron specific expression of *abi-1* in the ALM, suggesting that ABI-1 also functions cell autonomously in the ALM during this migration. Further investigation into the MIG-10/ABI-1 relationship was done by feeding RNAi of *abi-1* in a *mig-10(ct41)* mutant strain. The ALM migration was not more severely truncated in the double mutant, suggesting that MIG-10 and ABI-1 work in the same pathway. Taken together, this evidence supports a model where MIG-10 and ABI-1 work together autonomously within the ALM to promote migration.

Introduction

The human brain contains an intricate circuitry of neurons, which must be tightly coordinated throughout development for proper function. The human brain begins developing early in embryogenesis and continues the process throughout adolescence. Brain development begins when the neural progenitor cells, located in the ventricular zone, begin to differentiate during the third gestational week. These neural progenitor cells give rise to more than 100 billion neurons and glial cells through asymmetric division and differentiation (Stiles & Jernigan, 2010). Neurons, the information processing cells of the brain, must migrate during development to reach their final destination. One example of this migration occurs in the developing neocortex where neurons use the guidance of radial glial cells to migrate and organize into 6 layers. The migration of neurons in the cerebral cortex is often referred to as an inside-out migration because the neurons that migrate earliest form the deeper layers of the neocortex, while the neurons that travel later migrate past the deep layers to form the more superficial layers of the neocortex (Figure 1, Stiles & Jernigan, 2010).

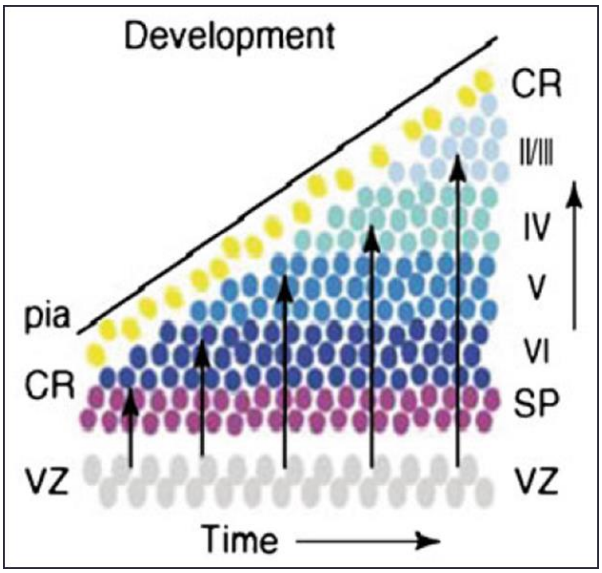

Figure 1: Migration of neurons in the neocortex. Early born neurons form the deeper layers of the neocortex while later born neurons form the more superficial layers. (Adapted from Cooper et al., 2008)

Similar to the neurons in the neocortex, a large majority of neurons in other areas of the brain will end up traveling away from where they were produced in the ventricular zone. Once migration is complete, each neuron can generate processes and make connections with other neurons. The connected neurons form the synapses necessary to complete the neuronal circuitry capable of effectively transmitting signals.

As described above, the process of neuronal migration is essential during nervous system development. Migration is typically initiated when an extracellular guidance cue binds to a receptor on the surface of a neuron triggering the downstream signaling pathways. These signaling pathways ultimately function to reorganize the cytoskeleton allowing the neuron's migration to be directed by the guidance cue in the direction of the guidance cue. Thus ensures that the migration occurs in the proper direction. Improper neuronal migration has been linked to various human disorders including lissencephaly, polymicrogyria, fetal cocaine syndrome, schizophrenia, and bipolar disorder (Valiente & Marin, 2010). Typically, these disorders begin during the mid-embryonic stages of development, are extremely devastating to the patient, and are mostly due to genetic causes. One of these diseases, lissencephaly, is characterized by the absence of folding in the cerebral cortex. This brain malformation is caused by genetic mutations, which cause the improper tangential and radial migration of neurons within the neoccortex, often resulting in early developmental delay and mental disabilities in children. Similarly, polymicrogyria is also the result of improper neuronal migration. In patients suffering from this disease, late-born neurons, which should migrate past the deeper layers of the neocortex to form the more superficial layers, accumulate in the deeper layers. This pathology is thought to be caused by defects in tubulin polymerization, which prevents the neuron from migrating. (Spalice et al., 2009; Valiente & Marin, 2010) Due to the severe developmental defects displayed in these diseases, the process of neuronal migration has been extensively studied. The guidance molecules and surface receptors that direct the migration of neurons have been well characterized through this research;

however, the cytoplasmic signaling systems which allow the cell to respond to these guidance cues are still not well understood. This study aimed to understand the function of two proteins, MIG-10/lamellipodin and ABI-1, which may participate in cytoplasmic signaling during neuronal migration.

C. *elegans* as a model system for studying neuronal migration

To investigate these cytoplasmic signaling systems, *C. elegans* was chosen as a model system. *C. elegans,* a transparent, microscopic, soil-dwelling nematode, contains a very simple nervous system with all of the neurons individually identified making it advantageous as a model system to investigate neuronal migration. *C. elegans* can be easily cultured in the lab as the animals feed on bacteria, have a relatively rapid life cycle of approximately 3 days, and can be maintained between 15- 20° Celsius. The *C. elegans* model system contains an extensive array of genetic tools, including a fully sequenced genome and the ability to label specific subsets of cells through the use of identified tissue specific promoters. RNAi is another well-established tool in *C. elegans*. Animals can ingest bacteria expressing double stranded RNA, which can trigger the mechanism of gene knockdown to occur systemically, in every cell of the organism. Gene knockdown and expression can also be performed cell specifically using transgenes. Transgenic lines can be maintained as an extra-chromosomal array or the array can be integrated into the genome. Because *C. elegans* is a self-fertilizing hermaphrodite with a small male population, recessive mutations can be easily maintained and crosses can be performed as well (Brenner, 1974; Wood, 1988).

The *C. elegans* nervous system contains only 302 neurons and 56 glial cells. Many of the neurons extend processes into a central nerve ring that surrounds the pharynx or bundles that run along the anterior-posterior axis of the animal (Harterink et al., 2011). Some C. *elegans* neurons, including three pairs of neurons, the HSN, CAN and ALM neurons, must migrate long distances during embryogenesis to their final positions in the mid-body. During these migrations, the neuron and axons are tightly positioned between the basal lamina and cell membrane of the epidermis (Fig. 2A). The HSN is

generated in the tail of the embryo and migrates anteriorly to its final location in the middle of the worm, while the CAN and ALM neurons migrate posteriorly from their original positions during embryogenesis (Fig 2B) (Altun, 2011. ; Hedgecock, 1987). The location and direction of these migrations can be seen in Figure 2.

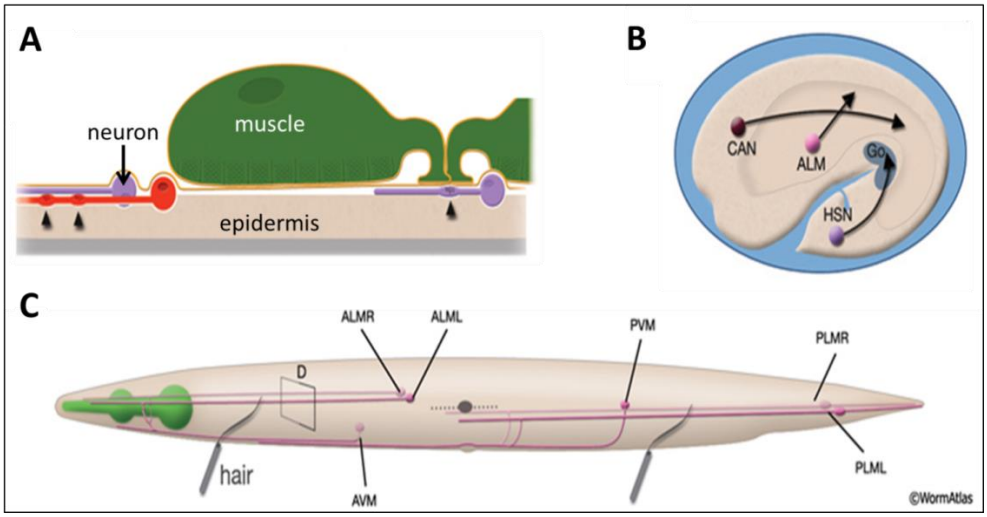

Figure 2: A. Neurons (purple and red) are positioned between the cell membrane and basal lamina (orange) of the epidermis. B. HSN migrates anteriorly while the CAN and ALM migrate posteriorly during embryogenesis. C. Final positions of the ALM neurons shown schematically in the mid-body of the adult animal. (Figure adapted from wormatlas.org)

For these neurons to migrate properly to reach their final location in the mid body, many cellular and molecular interactions are necessary to produce a change in cytoskeletal dynamics at the leading edge.

Guidance Cues Initiate Cellular Signaling in Neuronal Migration

During the initial step of the migration, the neuronal growth cone must respond to extracellular guidance cues, which can trigger signal transduction pathways and stimulate cytoskeletal rearrangements. There are four major types of guidance cues including Netrins, Slits, Semaphorins and Ephrins (Dontchev & Letourneau, 2003). These guidance cues are highly conserved and include some of the best studied molecules in the process of neuronal migration. All these families of guidance cues can participate in chemo-attraction or chemo-repulsion of a migrating cell or process. The method a

guidance cue utilizes will typically control the amount and type of receptors on the surface of the migrating cell. (Dontchev & Letourneau, 2003).

Netrins are a small family of conserved guidance cues capable of functioning at long range or short range depending on the specific conditions. The Netrin family contains one *C. elegans* homolog, UNC-6. The *unc-6* gene encodes for a Netrin protein that is localized at the ventral midline of the animal. This Netrin protein has been shown to be required for axon guidance along the dorsal ventral axis. The attractive effects of Netrins are mediated by the DCC family of receptors, including UNC-40, while the repulsive effects of Netrins are mediated by members of the UNC-5 family of receptors (Hall, 1990; Kolodkin & Tessier-Lavigne, 2011; Marc Tessier-Lavigne, 1988).

The SLIT family of guidance cues contains large secreted proteins. These proteins were first discovered to be involved in axonal repulsion in *Drosophila* and vertebrate systems. The SLIT family includes one *C. elegans* homolog, SLT-1. The repulsive actions of SLIT proteins are mediated by two receptors belonging to the Robo family. These two receptors are encoded by two splice variants of the *sax-3* gene in *C. elegans*. These receptors are similar to the receptors used by the Netrin family, as both types of receptors are members of the immunoglobulin superfamily. (Kolodkin & Tessier-Lavigne, 2011; Li HS, 1999).

The Semaphorins are a large conserved protein family that includes both secreted and transmembrane guidance cues which can operate as long range and short range guidance cues. The major receptors for Semaphorins are members of the Plexin family. Often the Semaphorins will act as inhibitory cues for axon guidance and migration (Kolodkin & Tessier-Lavigne, 2011; Yazdani & Terman, 2006).

The Ephrin family of guidance cues consists of cell surface signaling molecules, which play widespread roles during development, including a function during axon guidance. Ephrins can only

function as short range guidance cues because these proteins must be clustered together to activate their Eph family tyrosine kinase receptors. These guidance cues appear non-functional if released from the cell surface (Klein, 2004; Kolodkin & Tessier-Lavigne, 2011).

Multiple types of guidance cues must interact with one another *in vivo* to promote axon guidance. One example of multiple types of guidance cue interaction in *C. elegans* is demonstrated by the opposing gradients of SLT-1 and UNC-6. These guidance cues are both present along the dorsal ventral axis. SLT-1 is secreted from dorsal sources, while UNC-6 is secreted from ventral sources. These two guidance cues work together in the AVM axon, which is guided toward the ventral nerve cord in response to both the SLT-1 repellent and the UNC-6 attractant (Hedgecock, 1987; Quinn et al., 2006).

Along with the four main types of guidance molecules, there can be other types of extracellular cues that are involved in neuronal migration including morphogens. Morphogens includes members of the Wnt family of proteins that participate in many aspects of development, including cell fate determination, proliferation and migration (Harterink et al., 2011). *C. elegans* express five individual Wnt proteins. Three Wnt genes, *lin-44*, *egl-20,* and *cwn-1,* are primarily expressed in the posterior region of the animal forming a gradient, while the remaining two Wnt genes *mom-2* and *cwn-2* are expressed uniformly along the anterior posterior axis. The HSN, CAN and ALM neurons all migrate in a Wnt dependent manner (Silhankova & Korswagen, 2007; Zinovyeva, Yamamoto, Sawa, & Forrester, 2008; Zou, 2006). For example, the Wnt family member *egl-20*, which is heavily expressed in the tail region, has been shown to act as a chemo-repellent in directing the migrations of the HSN from its original position in the tail region to the final location in the mid-body of the animal (Pan et al., 2006). Wnt dependent migration is highly complex. *egl-20* single mutants display truncated HSN migration. However, *cwn-1; cwn-2* double mutants can also produce an HSN migration defect of similar severity. This demonstrates a role for multiple Wnts during the migration of a single neuron.

Molecular Mechanisms of Neuronal Migration

To be effective, the guidance cues that are detected at the cell surface must be transduced into localized remodeling of the cytoskeleton within the neuron. To further investigate the molecules participating in the process of migration, a screen was conducted to discover genes involved in the migration of the CAN neuron (Manser, Roonprapunt, & Margolis, 1997). One of the genes identified through this screen was *mig-10*.

The protein encoded by the *mig-10* gene, MIG-10, is a member of the MRL family of cytoplasmic adaptor proteins which includes human homologs lamellipodin and RIAM and the *Drosophila* homolog Pico (Colo, Lafuente, & Teixido, 2012). This family of proteins is involved in the regulation of actin dynamics, cell adhesion and migration. The MRL family of proteins shares an N-terminal coiled-coil region, a Ras association domain, a plextrin homology domain and a proline-rich C-terminal region (Fig. 3). The C-terminal region contains an FPPPP motif that can interact with Ena/VASP family members and an XPPP motif that can interact with profilin and SH3 binding motifs of other proteins (Colo et al., 2012). The *mig-10* gene encodes three alternatively spliced transcripts that only differ at the 5' ends and the three transcripts produce three distinct protein isoforms (Krause et al., 2004, Lafuente et al., 2004). The three isoforms of MIG-10 which are termed MIG-10a, MIG-10b and MIG-10c, (Fig 3), each contain all of the conserved domains discussed earlier and only differ in the length and sequence of the N-terminus.

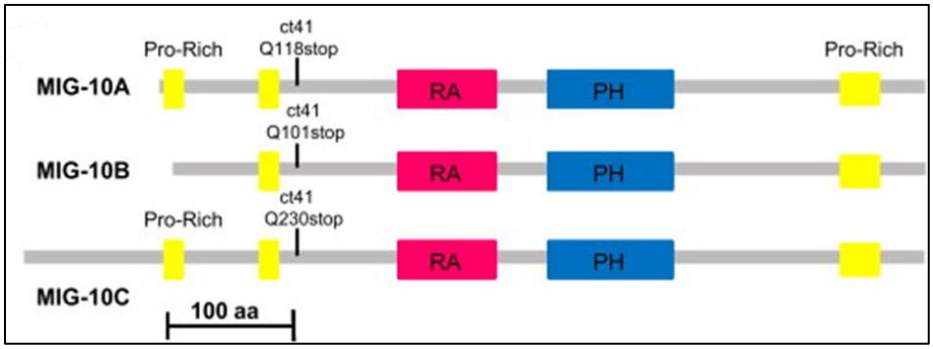

Figure 3: Model showing the three protein isoforms of *mig-10.*These proteins contain conserved Ras association and plextrin homology domains. The position of the stop codon that produces the null *mig-10(ct41)* mutation is shown on each isoform.

In the *mig-10(ct41)* mutant, a stop codon is predicted to prematurely truncate all three isoforms, which would prevent expression of the region containing the RA and PH domains (Manser et al., 1997). The *mig-10(ct41)* mutation acts as a null allele. *C. elegans* homozygous for the *mig-10(ct41)* mutation demonstrate truncation of the posterior migration of the CAN and ALM neurons and the anterior migration of the HSN. *mig-10* is involved in many other processes including axon outgrowth of the HSN, AVM and CAN, migration of the coelomocytes, and outgrowth of the excretory cell processes of the animal (Manser and Wood 1990).

In the ventral axon guidance of the AVM and PVM neurons, genetic analysis demonstrated MIG-10 functions downstream of the known guidance cues involved, UNC-6 and SLT-1 (Quinn et al., 2006; Chang et al., 2006). *mig-10* single mutants display no ventral guidance defect; however, the loss of MIG-10 and either the UNC-6 or SLT-1 guidance cues enhanced the defects in AVM and PVM axon guidance. Comparison of defects of the *mig-10; unc-6* guidance defect and *mig-10; slt-1* to the defect caused *by unc-6; slt-1* mutations suggests that MIG-10 functions downstream of both these guidance cues during AVM and PVM axon guidance (Quinn et al., 2006).

Overexpression of MIG-10 in absence of both the UNC-6 and SLT-1 guidance cues can create a multipolar phenotype in AVM and PVM neurons, which are normally monopolar. The presence of either one of the guidance cues can suppress the multipolar phenotype caused by MIG-10 overexpression (Quinn et al., 2006). The guidance defects displayed by *unc-6* and *sid-1* mutants were also reduced by the over expression if MIG-10. These results demonstrate that MIG-10 possesses outgrowth promoting activity that is not dependent on the UNC-6 or SLT-1 guidance cues (Quinn et al., 2006).

The evidence demonstrating the outgrowth promoting activity of MIG-10 in *C. elegans* is supported by the work in other model systems. Lamellipodin, the human homolog of *mig-10*, has been shown to localize to the tips of lamellipodia and filapodia in migrating fibroblasts cells (Krause et al.,

2004). In cell culture, overexpression of lamellipodin has been shown to increase the rate of lamellipodial protrusion, while the knockdown of lamellipodin expression inhibited the formation of lamellipodia. This work provided insight into a possible mechanism for how *mig-10* promotes axon and neuronal outgrowth. These results support a model where MIG-10 transduces instructions of the guidance cues within the cell.

To potentiate outgrowth promoting activity appropriately, MIG-10 must become asymmetrically localized to the leading edge of the migrating neuron in response to the guidance cues. In response to guidance cue binding, guanine nucleotide exchange factors become stimulated and can activate Rac. Rac is a small GTPase that has been implicated in axon guidance and is thought to be activated at the leading edge of the migrating cell (Lundquist et al. 2001, Ng et al., 2002). It has been shown that Rac acts downstream in the same pathway as the UNC-6 and SLT-1 guidance cues, suggesting that Rac could function in a pathway with UNC-6 to asymmetrically localize MIG-10. This model is further supported by evidence demonstrating that MIG-10 binds to activated Rac through the conserved Ras association domain. Additionally, a fragment of MIG-10 containing only the highly conserved RA and PH domain was sufficient to bind Rac *in vitro*. (Quinn, Pfeil, & Wadsworth, 2008) The *in vitro* studies have been supported by *in vivo* investigation. In *C. elegans*, the HSN axon migrates ventrally in response to the UNC-6 guidance cue. MIG-10 has been shown to accumulate on the ventral edge of the HSN cell body as this outgrowth and migration initiates (Adler, et al., 2006). The binding between CED-10, the *C. elegans* Rac homolog, and MIG-10 was shown to be essential for the localization of MIG-10 to the ventral edge of the HSN (Quinn, et al., 2008). These results suggest that Rac regulates the localization of MIG-10 to the leading edge of the migrating cell.

In other model systems, including neutrophils and Dictyostelium amoebae, investigation of lamellipodin regulators was conducted. Phosphoinositide-3- kinase (PI3K) was observed to define the

leading edge of migrating cells in each of these systems. This kinase stimulates the production of $PI(3,4)P_2$, which was shown to bind specifically to the conserved pleckstrin homology domain of lamellipodin (Krause et al., 2004). This implicates a role for PI3K and $PI(3,4)P_2$ in the process of neuronal migration. The *C. elegans* PI3K homolog, AGE-1, can suppress the excessive outgrowth phenotype of MIG-10 overexpression suggesting that these proteins are involved in the same pathway during the axon outgrowth and neuronal migration. (Chang et al., 2006). In addition, mutation of *age-1* affected the accumulation of MIG-10 at the ventral side of the HSN cell body. Analysis of *ced-10*; *mig-10* and *age-1*; *mig-10* double mutants showed no enhancement of axon defects in the AVM relative to the single mutants (Chang et al., 2006). These results point towards a model where guidance cues stimulate GEFs which activates Rac and stimulates PI3K to produce $PI(3,4)P_2$ at the leading edge of the migrating cell (Fig 4A). MIG-10 can then associate with these molecules through the Ras association domain and pleckstrin homology domain. Association of MIG-10 to these proteins localizes MIG-10 to the leading edge.

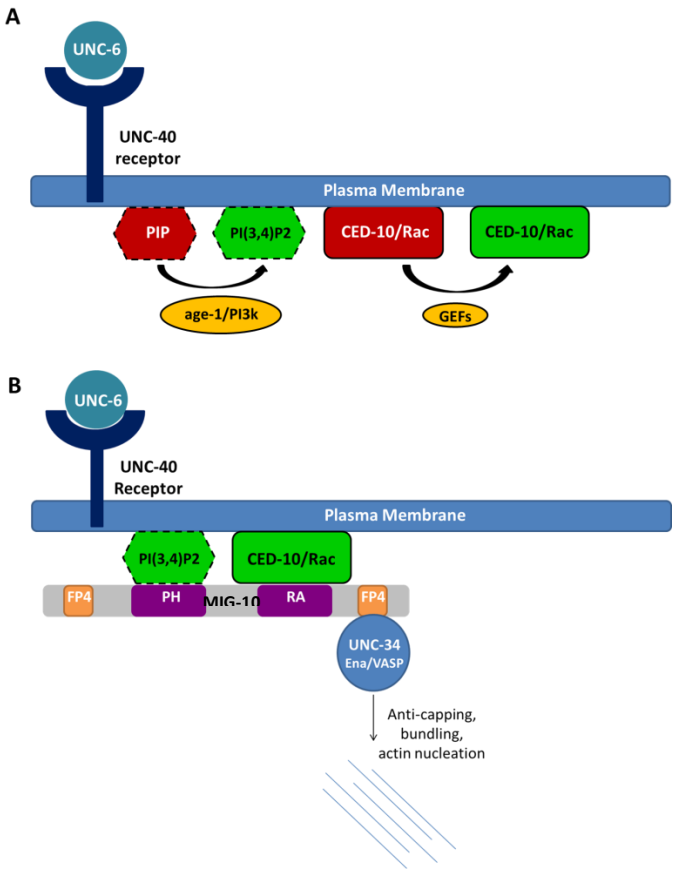

Figure 4: Model representing a possible mechanism for the asymmetric recruitment of MIG-10 during axon guidance.

Once MIG-10 has been localized to the leading edge, it can recruit members of the actin polymerization machinery to carry out its outgrowth promoting activity (Fig 4B). Lamellipodin and MIG-10 each contain an FPPPP motif, which have been shown to bind to Ena/VASP family members through the conserved EVH1 domains (Quinn et al., 2006; Krause et al., 2004). These Ena/VASP proteins are active in many different cell types such as fibroblasts, endothelial cells, epithelial cells, and neurons and are known to regulate assembly and remodeling of the actin cytoskeleton (Bear & Gertler, 2009). Ena/VASP promotes the formation of filopodia by preventing the capping of actin filaments (Barzik et al., 2005; James E. Bear, 2002). Ena/VASP have also been shown to promote filapodia formation by reducing the function of Arp2/3 in actin filament branching and supporting the clustering of filaments at the tips of actin (Applewhite et al., 2007; James E. Bear, 2002).

Similar to the localization patterns of lamellipodin and MIG-10, Ena/VASP proteins are concentrated at the tips of lamellipodia and filapodia in migrating cells (Bear, et al., 2002). Lamellipodin has been shown to bind to Ena/VASP proteins *in vitro* and *in vivo* through the EVH1 domain. The localization of the Ena/VASP proteins is dependent on functional Lamellipodin suggesting lamellipodin recruits Ena/VASP to the leading edge (Krause et al., 2004). *C. elegans* contain only one Ena/VASP family homolog, UNC-34. Null mutations in *unc-34* cause defects in axon guidance and neuronal migration of several neurons, including the CAN neuron (Fleming et al., 2010). Mutations causing deletion of the EVH1 domain are equally as severe as the null mutations during neuronal migration of the CAN neuron. These results suggest that the EVH1 domain of UNC-34 is essential for the proper migration to occur. This suggests that similar to the relationship of lamellipodin and Ena/VASP, MIG-10 can localize UNC-34 to the leading edge by binding the EVH1 domain during neuronal migration (Fleming et al., 2010). Once localized, UNC-34 can perform its function though anti-capping and anti-branching of the actin filaments causing them to polymerize in the proper direction.

However, UNC-34 cannot be the only mediator of the outgrowth activity of MIG-10. Evidence shows that *unc-34* null mutations have no effect on the excessive outgrowth phenotype caused by MIG-10 overexpression. If UNC-34 was carrying out all of the outgrowth activity then removing the UNC-34 protein should suppress the effects of MIG-10 overexpression. Also, the *mig-10*; *unc-34* double mutant produces a much more severe phenotype than either single mutant (Chang et al., 2006). If UNC-34 was the only effector working in the same pathway as MIG-10, then it would be hypothesized that there would be no enhancement of the ALM migration defect when both proteins were non-functional. However, if these two proteins are acting in parallel pathways, an enhancement of the migration defect would be expected. Additionally, in fibroblasts, the loss of Ena/VASP does not cause the complete loss of the F-actin at the leading edge that is seen in lamellipodin mutants (Krause et al., 2004). If UNC-34 is the only mediator of the outgrowth promoting ability of MIG-10, each of these single mutants should

produce the same effects on the F-actin suggesting a model in which MIG-10 and UNC-34 function in parallel or overlapping pathways. Taken together, these results suggest that MIG-10 must interact with other mediators, which control cytoskeletal dynamics.

MIG-10 may function with ABI-1 during neuronal migration and outgrowth

To identify the other proteins that may bind to MIG-10 to help facilitate actin polymerization, a yeast-2 hybrid screen was performed, using MIG-10a as bait. Twenty-eight MIG-10 interactors were identified, the strongest of which was ABI-1 (McShea et al., 2013). This screen was confirmed by a concurrent study which used an RNAi sublibrary of genes that contained polyproline binding domains. This sublibrary was used to screen for phenotypes similar to the loss of *mig-10.* This screen also identified ABI-1 as a potential mediator of the outgrowth promoting activity of MIG-10 (Xu & Quinn, 2012).

ABI-1 is a conserved protein with homologs in *Drosophila*, mouse and human. ABI-1 was discovered as a target of the abelson tyrosine kinase, ABL, which is a regulator of cytoskeletal dynamics (Shi, et al. 1995, Lanier & Gertler, 200). ABI-1 is a member of the WAVE regulatory complex, which is involved in a number of cellular processes including cell adhesion, communication, division, and migration. Due to the complex's involvement in many different developmental processes, ABI-1 is expressed in many cell types, including many neurons (Patel, et al, 2008, Schmidt, et al., 2009). The WAVE complex has been shown to participate in remodeling the actin cytoskeleton through the Arp2/3 complex which functions in nucleation and branching of actin filaments. All components of the WAVE complex, including *gex-2*, *gex-3*, *abi-1* and *wve-1*, contribute to actin nucleation dependent migration. The loss of any of these components causes embryonic lethality because the epidermis cannot migrate properly (Patel et al., 2008). The WAVE complex and ABI-1 specifically has been shown to localize to the tips of lamellipodia and filopodia of migrating cells (Patel et al., 2008).

The *abi-1* gene consists of 5 exons and encodes a single protein isoform. The ABI-1 protein contains a conserved Q-snare domain and abelson homeodomain homology region at the N-terminus, a serine rich region in the center and an SH3 domain at the C-terminus of the protein (Fig 5).

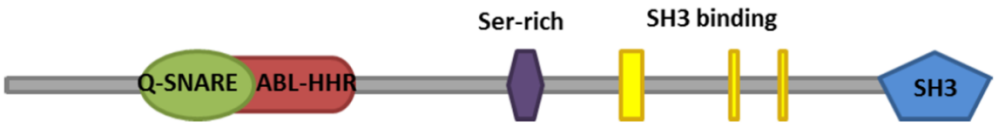

Figure 5: Schematic of ABI-1 domains. These domains include a Q-SNARE and ABL-HHR domain at the N terminus of the protein and an SH3 domain at the C-terminus (Adapted from Schmidt et al., 2009).

The abelson homeodomain homology region is the defining feature of all proteins capable of interacting with Abelson family tyrosine kinases. The N-terminus of the mammalian ABI protein has been shown to bind the WVE-1 protein, while the SH3 domain participates in ABI-1 binding to ABL (Echarri, Lai, Robinson, & Pendergast, 2004). The interaction between ABI-1 and MIG-10 was confirmed by co-immunoprecipitation and the SH3 domain was also found to be essential for binding to occur between these two proteins (McShea et al., 2013).

Interaction of MIG-10 and ABI-1 was initially shown to be important in axon guidance and synaptic vesicle clustering through analysis of *mig-10(ct41); abi-1(tm494)* transheterozygotes. In *C. elegans*, the only available non-lethal mutation in *abi-1*, *abi-1(tm494)*, is a weak loss of function mutation. This mutation causes a frame shift, beginning in exon four, which is thought to create a shortened protein with deletion of the SH3 domain. *mig-10(ct41)* and *abi-1(tm494)* are both recessive loss of function mutations; however mutating one allele of each gene in the same animal causes defects in axon guidance and synaptic vesicle clustering (Stavoe et al., 2012). This suggests that MIG-10 functions with ABI-1 during these processes. This conclusion is also supported by evidence demonstrating that *abi-1* mutants can suppress the axon guidance defects caused by overexpression of the UNC-40 receptor (Xu & Quinn, 2012). This places ABI-1 downstream of UNC-6, which is the guidance

cue capable of binding the UNC-40 receptor. This evidence suggests that ABI-1 can respond to the same guidance cues as MIG-10, suggesting they may function together during this process.

During excretory canal outgrowth, *abi-1(RNAi)* greatly enhanced the outgrowth defect caused by the *mig-10(ct41)* mutation, suggesting that ABI-1 and MIG-10 can also function in separate pathways (McShea et al., 2013). However, evidence from mammalian cell culture demonstrates that MIG-10 and ABI-1 work together to reorganize the actin cytoskeleton. In these cultured cells, expression of *mig-10* induces the formation of lamellipodia. The amount of lamellipodia can then be reduced by knocking down expression of *abi-1* through shRNA (Xu & Quinn, 2012).

It has been shown that MIG-10 and ABI-1 act together during axon guidance. Although many genes and functions are conserved in axon guidance and neuronal migration there are also differences. For example, the effects of *mig-10* mutations on migration are much more pronounced than those on axon guidance. Evidence consistent with MIG-10 and ABI-1 acting in the same pathway, demonstrated that the weak loss of function mutation of *abi-1(tm494)* causes migration defects similar to the defects recorded from the null *mig-10(ct41)* mutant (McShea et al., 2013). *However, it has not been shown whether MIG-10 and ABI-1 act in the same pathway during neuronal migration or whether these proteins act in the neurons, epidermis or both cell types.* This work was conducted to test the model where ABI-1 functions as an additional mediator of MIG-10, along with UNC-34, to promote outgrowth during neuronal migration.

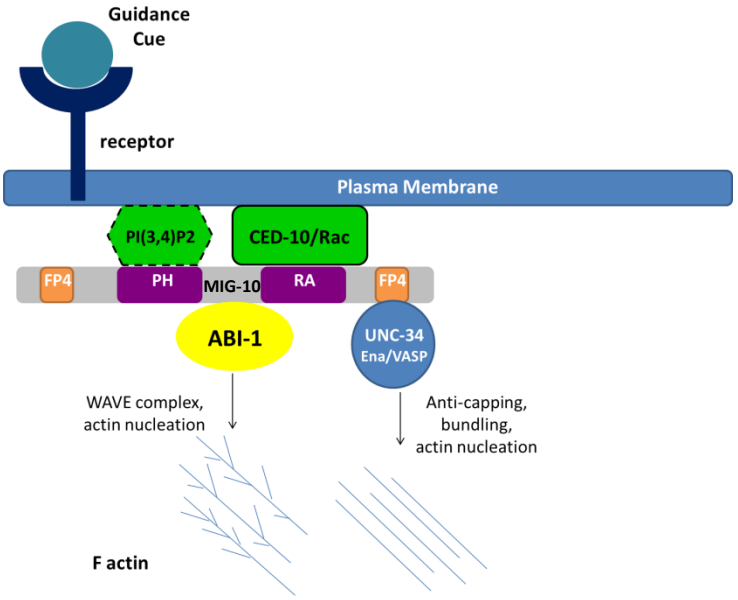

Figure 6: Proposed model for *C. elegans* neuronal migration. This model proposes that binding of extracellular guidance cues cause the asymmetric localization of MIG-10 which recruits UNC-34 and ABI-1 to initiate cytoskeletal remodeling.

Project Goals

There are two possibilities for how the interaction between MIG-10 and ABI-1 may occur. During migration, neurons travel tightly positioned between the basal lamina and the underlying epidermal seam cells(Hedgecock, 1987). It is possible that MIG-10 and/or ABI-1 may function in the underlying cells or in both cell types during ALM migration. Early evidence from mosaic analysis supported a non-autonomous function for MIG-10 during excretory cell outgrowth (Manser et al., 1997). Also, there is evidence that axon outgrowth may require some non-autonomous signaling to produce the extracellular matrix cues needed for the axon to reach its target properly (Hannes E. Bulow, 2004). Alternatively, it is possible that both MIG-10 and ABI-1 function autonomously in the ALM to promote migration. This mechanism is supported by evidence showing that ABI-1 acts cell autonomously during the process of axon guidance(Xu & Quinn, 2012).

- To determine if MIG-10 and ABI-1 function cell autonomously, cell specific rescue and RNAi experiments were performed.

- To investigate whether *mig-10* and *abi-1* are acting in the same pathway, *mig*-10*(ct41)* mutant animals and wild type animals fed *abi*-1*(RNAi)* were compared to *mig*-10*(ct41)* animals fed *abi*-1(*RNAi).*
    - If these proteins are acting in the same pathway, then no enhancement would be expected by knocking down both of these proteins. However, if acting in parallel pathway knocking down expression of both proteins would enhance the migration defects when compared to each single knockdown.
- *abi-1(RNAi)* was also performed in the underlying epithelial cells to determine whether there is any non-autonomous function *abi-1*.

Methods

C. elegans neuronal migration measurements

Animals were washed off the plate using M9 buffer. The animals were pipetted into an Eppendorf tube using a Pasteur pipette and allowed to settle to the bottom of the tube. Once settled 5µl of the liquid containing the animals was pipetted from the bottom of the tube onto a glass slide with a 2% agarose + 10 mM NaN_3 .A coverslip was placed on the slide and the animals were visualized using a Zeiss compound microscope equipped with epifluorescence. Images of L4 animals were taken and imported into the ImageJ software program. The position of each neuron was measured in reference to the posterior bulb of the pharynx or to the vulva (Figure 7). The ALM neurons, which migrate posteriorly, were measured from the posterior bulb of the pharynx to the cell body. The measurement from each ALM cell body to the pharynx was average for the two ALM neurons and then normalized by dividing by the total distance from the pharynx to the vulva. The AVM neuron, which migrates anteriorly, was measured from the vulva to the AVM cell body and then normalized by dividing by the total distance from the pharynx to the vulva (Fig. 7).

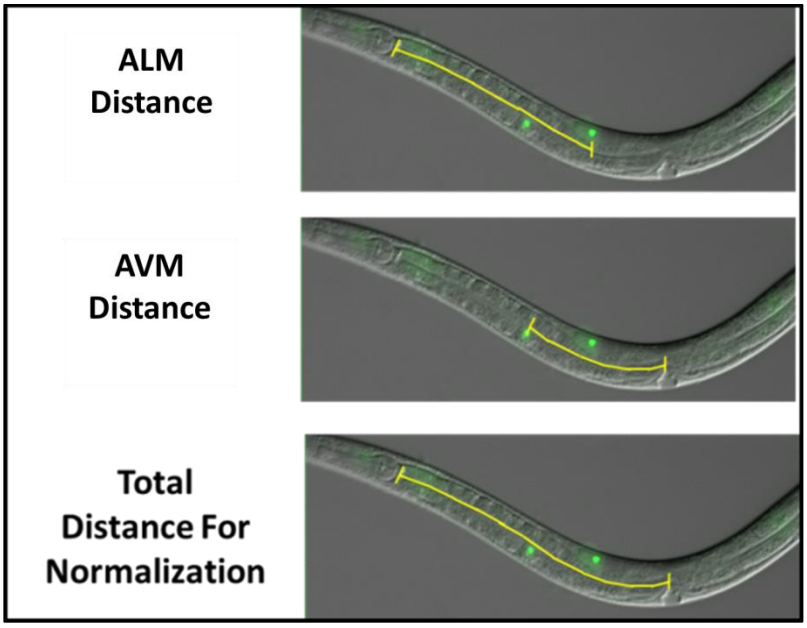

Figure 7: Method used to quantify neuron migration. The distance of each neuron from a reference point was measured and then divided by the total distance to normalize for the size of the animal.

Molecular Biology

PCR

PCR of all fragments used in cloning was performed using approximately 400ng of the original template. The template was combined with 5 units of TakaRa Ex-Taq Polymerase, Ex-Taq Buffer plus (includes 20mM Mg^{2+}), 5uM pf each primer and 2.5mM dNTP mixture. A 50µl reaction was set up for each PCR following the formula below.

Reaction Components	Stock concentration	Volume per Reaction
TaKaRa Taq	5units/µl	0.25 µl
10x Ex-Taq Buffer	10x	5 µl
dNTP	2.5mM	4 µl
Original vector template	<500ng	2 µl
Forward Primer	5µM	5 µl
Reverse Primer	5µM	5 µl
dH_2O	-	28.75 µl

Figure 8: Formula for 50µl TakaRa PCR reaction used to produce A-tailed PCR products.

Each PCR reaction was run according to the reaction conditions suggested by the TaKaRa Ex-Taq polymerase standard protocol. The reaction was run at 98°C for 10 seconds, followed by 55°C for 30 seconds and then 72°C for 1 minute per 1kb of the fragment being amplified. These settings cycled 30 times and then the reaction was held at 4°C when completed.

The primers used to generate the PCR fragments used in cloning are listed in Figure 9.

Forward Primer	Reverse Primer	Template Vector	Fragment Amplified
TCGCTATCAAGTTATAGAGT TGCG	GGACTTAGAAGTCAGAGG CAC	*pttx-3:abi-1*:GFP	*abi-1* antisense
GCGATAGCATGCGAATTCA CAGTTTACCAAACTAG	GCGATAGCTAGCGCTTCCT TCCTTCGGTGAGGCG	*pdlg-1:dlg-1*	*dlg-1* promoter
GCGATAGCTAGCGAAGCTC TTGAAACTCAACTCAACTC	GCGATAGGTACCATTGACT TCACATTTTCCCGGCTAG	*pmec-4:mig-10a*	100bp *mig-10* sense
GCGATAGCTAGCATTGACTT CACATTTTCCCGGCTAG	GCGATAGGTACCGAAGCTC TTGAAACTCAACTCAACTC	*pmec-4:mig-10a*	100bp *mig-10* antisense

Figure 9: Primers used to generate A-tailed PCR products used for ligation into the PGEM T-Easy Vector.

Gel Extraction, Ligation, Transformation, DNA isolation

After PCR or restriction digest, DNA fragments were run on a 0.8% agarose gel in TAE buffer. Desired fragments were subsequently gel extracted using the QIAquick Gel Extraction Kit (Qiagen). Purified DNA being ligated into the pGEM T-easy vector was ligated using a 10µl reaction including a 1x ligation buffer, 3 Weiss units of T4 DNA ligase (provided by the Promega pGEM kit), nuclease free dH_20 and the purified vector and insert DNA. The vector and insert DNA was added to the reaction at a 2:1 molar ratio with the total DNA concentration totaling <100ng/µl. The ligation reaction was incubated at 16° C overnight. The same protocol was followed for all other ligations of vector and insert however commercially available T4 DNA ligase was used.

4µl of the ligation reaction was added to 50µl of Maximum-efficiency DH5a *E. coli* chemically competent cells (New England Bioloabs) and incubated on ice for 30minutes. After incubation the cells were heat shocked at 42°C for 30 seconds and then allowed to recover in 400µl SOC medium at 37° C for 1-3 hours. After 12-15 hours, aliquots of 50µl and 150µl of these transformed cells were spread onto LB agar plates containing 50µg/mL ampicillin. The plates were incubated overnight at 37° Celsius. After 12-15 hours, bacterial colonies were picked into a 15mL conical tube containing LB liquid media with

50µg/mL ampicillin using a pipette tip and grown overnight at 37° C. The DNA was isolated using the QIAprep Spin Miniprep Kit (Qiagen) and accompanying protocol.

Construction of final plasmids

The construct designed for expression of *abi-1*:gfp in the mechanosensory neurons was generated by swapping the 1.2kb *mec-4* promoter sequence from the *mec-4:mig-10a* vector (provided by C. Quinn, U Wisconsin-Milwaukee) for the *ttx-3* promoter from the *ttx-3:abi-1*:GFP plasmid (provided by D. Colon-Ramos, Yale)(Fig. 10). This was done by digestion of each vector with Sph1-HF and Nhe1-HF restriction enzymes to separate the vector and insert of each original plasmid. The *mec-4* promoter and *abi-1*:GFP vector backbone was isolated though gel extraction using the QIAquick Gel Extraction Kit (Qiagen). The purified DNA was ligated and transformed as previously described. The *mec-4:abi-1*:GFP plasmid was isolated using the QIAprep Spin Miniprep Kit (Qiagen) protocol. The presence and size of the plasmid was confirmed through restriction digest with Sph1-HF and Nhe1-HF, followed by gel electrophoresis using a 0.8% agarose gel in TAE buffer. The *mec-4* promoter region, the *abi-1* cDNA, and the GFP fusion portion of the vector were all confirmed by sequencing analysis.

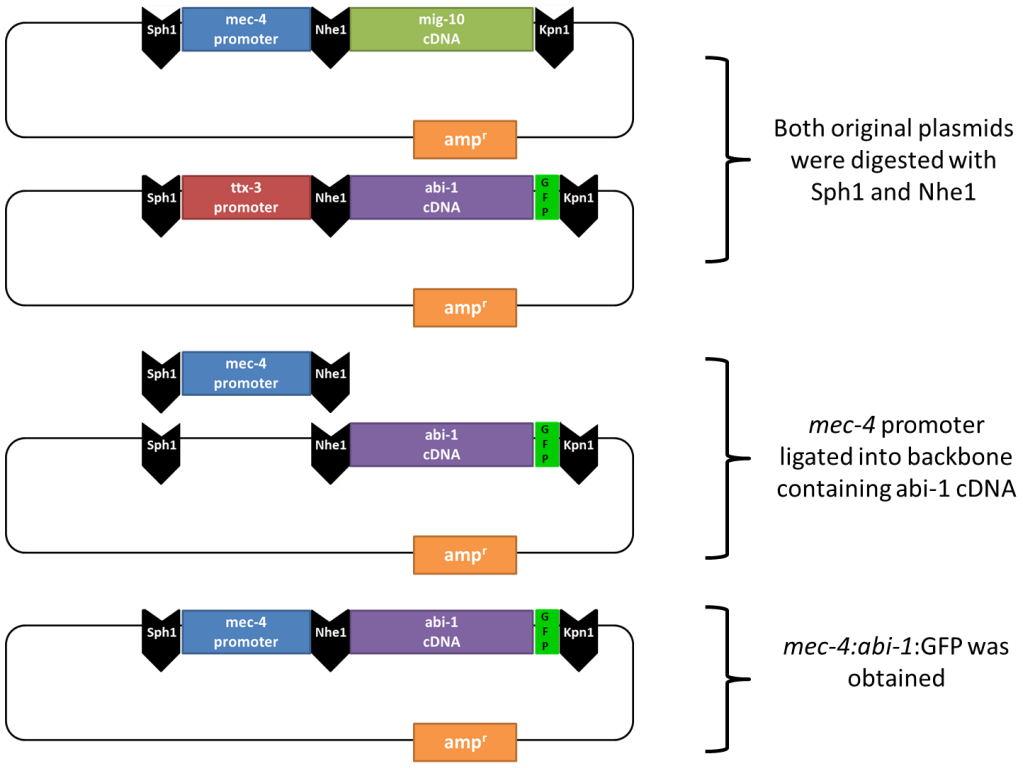

Figure 10: Strategy used to clone the *mec-4* promoter into the *abi-1*:GFP vector backbone. This strategy produces a plasmid designed for neuron specific expression of *abi-1* cDNA

To design the *mec-4:abi-1* antisense construct, the *abi-1* cDNA was directionally cloned into the *mec-4:mig-10a* vector (Fig. 11) . Primers were designed to flank the 5' and 3' end of the cDNA with Nhe1 and Kpn1 restriction sites respectively. The PCR product was gel purified using the QIAquick Gel Extraction Kit (Qiagen) and then ligated into the pGEM T-easy Vector (Promega) as previously described. The QIAprep Spin Miniprep Kit (Qiagen) was used to isolate the pGEM T-easy vector containing the *abi-1* antisense plasmid DNA. The presence and size of the plasmid DNA was confirmed through restriction digest with Nhe1-HF and Kpn1-HF, followed by gel electrophoresis using a 0.8% agarose gel in TAE buffer. The *abi-1* antisense fragment was also confirmed through sequencing analysis. The *abi-1* antisense fragment was then excised from the pGEM T-easy vector by digestion of the DNA with Nhe1-HF and Kpn1-HF. The digested vector and insert were separated on a 0.8% agarose gel in TAE and the *abi-1* antisense fragment was purified using the QIAquick Gel Extraction Protocol. The *mec-4:mig-10a*

backbone was digested and purified in the same manner. The *abi-1* antisense fragment was ligated into the *pmec-4* vector backbone was transformed, miniprepped, and analyzed by restriction digestion as previously described. The same cloning strategy was used to clone 100bp fragments of *mig-10* from *mec-4:mig-10a* plasmid into a vector backbone containing *mec-4*. This strategy created *mec-4:mig10*(100bp) and *mec-4:mig-10*(100bp) antisense plasmids. (Cloning performed by Rebekah Cocks)

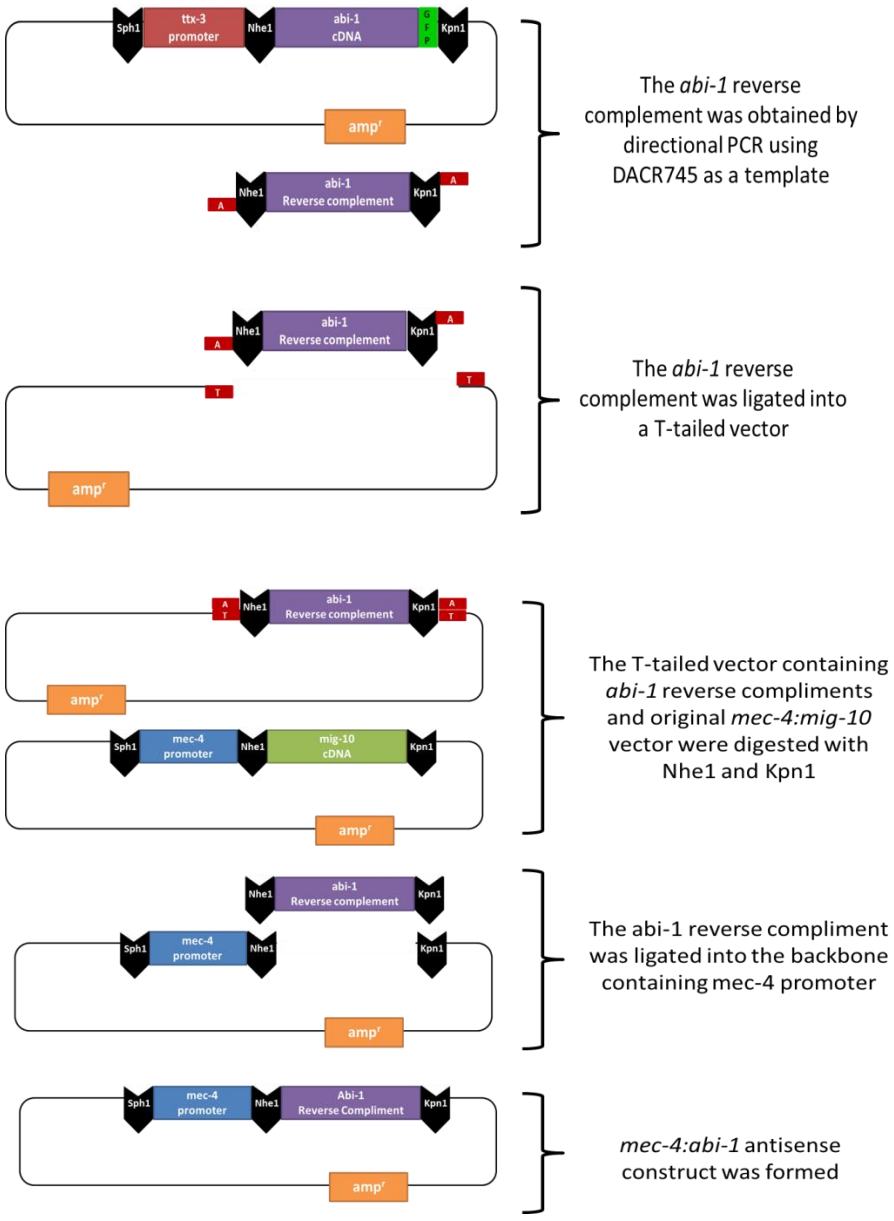

Figure 11: Strategy used to obtain the *abi-1* antisense cDNA and clone the *abi-1* antisense cDNA into the *pmec-4* vector backbone. The final construct was designed to produce neuron specific expression of *abi-1* antisense.

To create the *dlg-1:abi-1*:gfp and *dlg-1:abi-1* antisense constructs the *dlg-1* promoter was PCR amplified from the *pdlg-1:dlg-1* vector (provided by C. Rongo, Rutgers University) using primers flanking the 5' and 3' ends with Sph1 and Nhe1 sites added respectively. The purified PCR product was ligated into the pGEM T-easy Vector (Promega) and the ligation was transformed, miniprepped, analyzed, and sequenced as described previously. The fragment was excised from the pGEM T-easy Vector by digestion with the Sph1-HF and Nhe1-HF restriction sites. The digested vector and insert were separated on a 0.8% agarose gel in TAE buffer and the inserts were purified using the QIAquick Gel Extraction Kit (Qiagen) The *mec-4:abi-1*:gfp and *mec-4:abi-1* antisense backbones were digested and purified using the same method. The insert was ligated into each vector at a 1:2 molar ratio of vector to insert and incubated overnight at 16° C. The ligations were transformed, miniprepped and analyzed for presence and size as described previously.

The *mec-4:mig-10* sense and antisense constructs were created by directional PCR of 100bp fragments of the *mig-10* cDNA from *the mec-4:mig-10a* construct.

Feeding RNAi

RNAi plates were produced from NGM agar, with IPTG and carbenicillin being added after the liquid media had cooled from autoclaving. The IPTG was added to produce a final concentration of1 mM and carbenicillin was added to produce a final concentration of 25µg/µl. Plates were poured to contain 10mL of media each, allowed to set and then stored at 4° C to prevent IPTG degradation. These plates were stored for a minimum of 3 days before use.

The RNAi bacterial strains were streaked on to LB plates containing 50µg/mL ampicillin and 12.5µl/mL TET and allowed to grow overnight at 37° C. Single colonies were picked into 15mL conical tubes containing 5mL LB and 50µg/mL ampicillin using a sterile pipet tip. The inoculated cultures were grown at 37° C for 12-15hours. After the incubation, the cultures were spun at 1400*g for 4 minutes and

all but 1mL of the supernatant was decanted. The bacterial pellet was re-suspended in the remaining 1mL of media and seeded onto the appropriate RNAi plate by applying 3-5 drops of cultured bacteria to the plate using a sterile Pasteur pipet. The plates were allowed to dry in the sterile hood overnight. After approximately 24-30 hours, 4-6 *C. elegans* in the L4 stage were transferred onto the seeded RNAi bacterial plates. After this transfer, plates were stored at 20° C for approximately 30 hours. After this time, the adult *C. elegans* on the primary plates were transferred onto a secondary plate that had been prepared in advance using the method previously described. Following transfer, the primary and secondary plates were stored at 20° C for about 72 hours. After this time the migration of the ALM and AVM neurons of the F1 progeny, which would be in the L4 stage of development, was quantified. This protocol was closely adapted from the methods described by Dubuke and Grant (Dubuke & Grant, 2009).

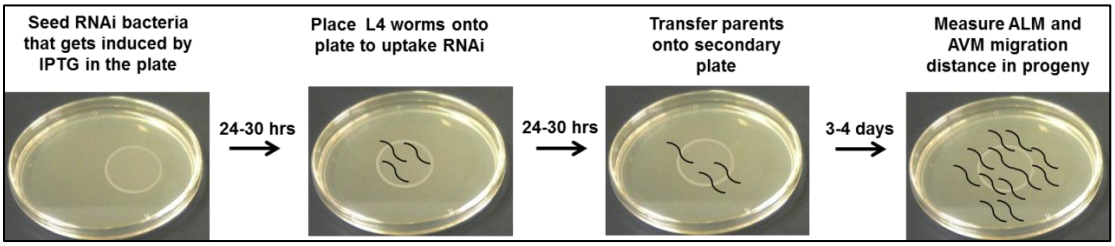

Figure 12: Graphical depiction of the RNAi feeding protocol.

Microinjection

To prepare for injection 2% agarose pads were made on cover glass and heated at 50°C for 2 hours. Glass capillaries were pulled on a Sutter micropipette puller using the settings as follows; Heat= 865, Velocity=50, Pressure= 60 and Time=160. A mixture of the plasmid and co-injection marker DNA was prepared to produce a total concentration of 200ng/µl and centrifuged at 13,000RPM for 10 minutes to remove any particulate. The DNA was loaded into the needle using a pulled 1 mL syringe and the needle tip was broken under the microscope.

Young adult hermaphrodites, preferably containing a single row of eggs were mounted in a drop of halocarbon oil on the 2% agarose pads. Animals were gently smoothed onto the 2% agar pad using a paint brush hair until the animal could no longer move. The distal gonad arm of the animal was injected with the appropriate DNA mixture under the microscope. After injection, the animal was recovered in 5µl of M9 buffer solution and picked from the buffer to an NGM plate seeded with OP50 *E. coli* bacteria. The injected animal was placed at 20° C for approximately 4 days post-injection. The F1 progeny were examined under florescent stereoscope for the presence of the co-injection marker which was either *unc-122:RFP* coelomocyte marker or the *ttx-3:mcherry* marker. Animals expressing the co-injection marker were picked singly onto individual seeded plates. The progeny of these singled animals were once again examined for the co-injection marker to determine if a stable line had been established (Fig. 13).

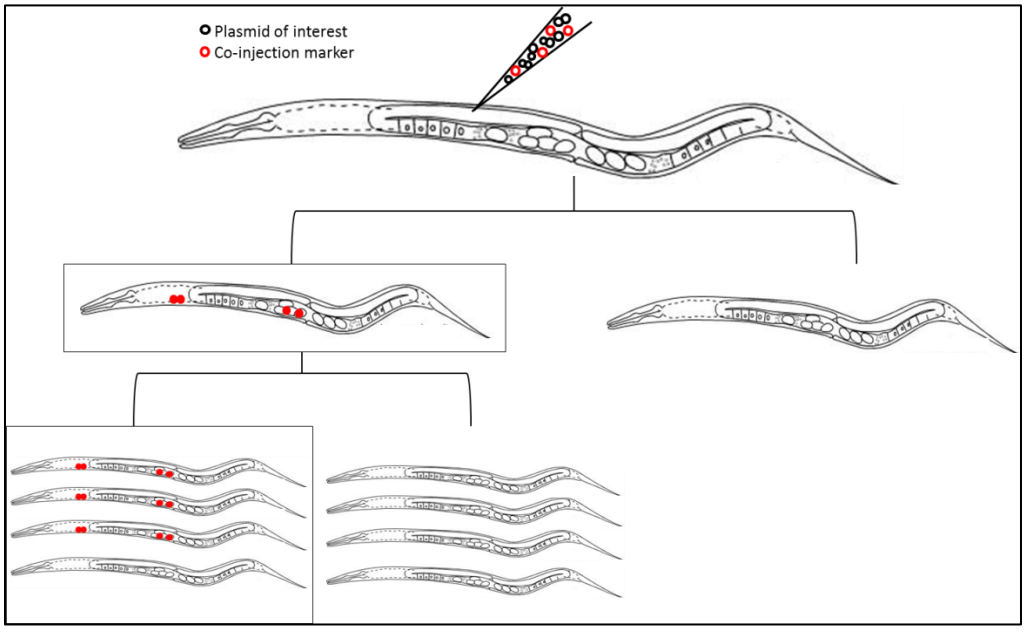

Figure 13: Protocol for establishing transgenic lines. Young adult animals injected with plasmid DNA along with unc-122:RFP which labels the coelemocytes is depicted. After injection, animals expressing the co-injection marker were singled onto a seeded plate. If the progeny also express the co-injection marker then a transgenic line was established. Importantly not all progeny in the transgenic line will express the extra-chromosomal array.

The strains created by microinjection can be seen in the Table below (Table 1).

Injection Strains		
Strain name	**Array**	**Array Concentration (ng/µl)**
RY1301 ynIS54;mpEx1301	mpEx1301[pttx-3:mcherry; punc-122:RFP]	100
RY1302 abi-1(tm494); mpEx1302; pgp-12:GFP	mpEx1302[punc-122:RFP;pmec-4:abi-1:GFP]	100
RY1303 abi-1(tm494); mpEx1302; pgp-12:GFP	mpEx1303[punc-122:RFP;pmec-4:abi-1:GFP]	100
RY1304 ynIS54;mpEx1304	mpEx1304 [punc-122:RFP; pmec-4:abi-1antisense]	50
RY1305 ynIS54;mpEx1305	mpEx1305 [pttx-3:mcherry; pmec-4:abi-1antisense]	100
RY1306 abi-1(tm494); ynIS54; mpEx1306	mpEx1306[pttx-3:mcherry;pmec-4:abi-1:GFP]	100
RY1307 ynIS54; mpEx1307	mpEx1307[punc-122:RFP;pmec-4:abi-1:GFP]	100
RY1308 ynIS54; mpEx1308	mpEx1308[punc-122:RFP;pdlg-1:abi-1:antisense]	100
RY1309 ynIS54; mpEx1309	mpEx1309[punc-122:RFP;pdlg-1:abi-1antisense]	100
RY1310 mig-10(ct41); ynIS54; mpEx1309	mpEx1309[pttx-3:mcerry;pmec-4:abi-1antisense]	100
RY1311 ynIS54;mpEx1310	mpEX1310 [punc-122:RFP;pmec-4:M5S; pmec-4:M5A]	50
RY1312 ynIS54; mpEx1311	mpEX1311 [punc-122:RFP;pmec-4:abi-1:GFP;pmec-4:abi-1 antisense]	50

Table 1: Strains created through microinjection. The strain name and genetic background are shown in the first column.ynIS54 is an integrated *pflp-20*:GFP transgene used to label the ALM and AVM neurons. The array and the concentration the array was injected are shown in the second and third columns respectively. The co-transformation marker was always included at a concentration to make the total 200 ng/µl

Results

MIG-10 and ABI-1 proteins could act to promote neuronal migration either in the migrating ALM and AVM neurons or in the underlying epidermal cells, or both cell types. To distinguish between these mechanisms, cell specific expression of *mig-10* and *abi-1* cDNA was performed in *mig-10(ct41)* and *abi-1(tm494)* mutants respectively. To confirm the cooperation of MIG-10 and ABI-1 in neuronal migration, *abi-1(RNAi)* knockdown was performed in a *mig-10(ct41)* mutant background. If the proposed model of MIG-10 localizing members of the actin polymerization machinery, specifically ABI-1, is supported, then there should be no enhancement of the migration defects displayed by the *mig-10(ct41)* mutant. Additionally, if recue can be performed cell autonomously, cell autonomous knockdown should also be possible for further support. Finally, to determine if the interaction of MIG-10 and ABI-1 is important in AVM migration, the AVM neuron was quantitated during each experiment.

mig-10 acts autonomously in the ALM neurons

To determine where expression of *mig-10* was required to rescue migration, *mig-10a* was expressed specifically in the ALM neurons or in underlying epidermis, and the location of the ALM neurons in larval animals was quantitated. In previous work, *mig-10(ct41)* mutant strains were injected with either *mec-3::mig-10a* to allow neuronal expression, or *dyp-7::mig-10a* to allow epidermal expression. Each construct was co-injected with *flp-20::GFP* to label the mechanosensory neurons, including the ALM neurons. These strains were compared to *mig-10(ct41)* mutant and wild type strains carrying an integrated *flp-20::GFP*. To allow consistent measurements, the final position of the ALM neurons after migration was complete was quantified at larval stage 4; the migration is completed during embryogenesis.

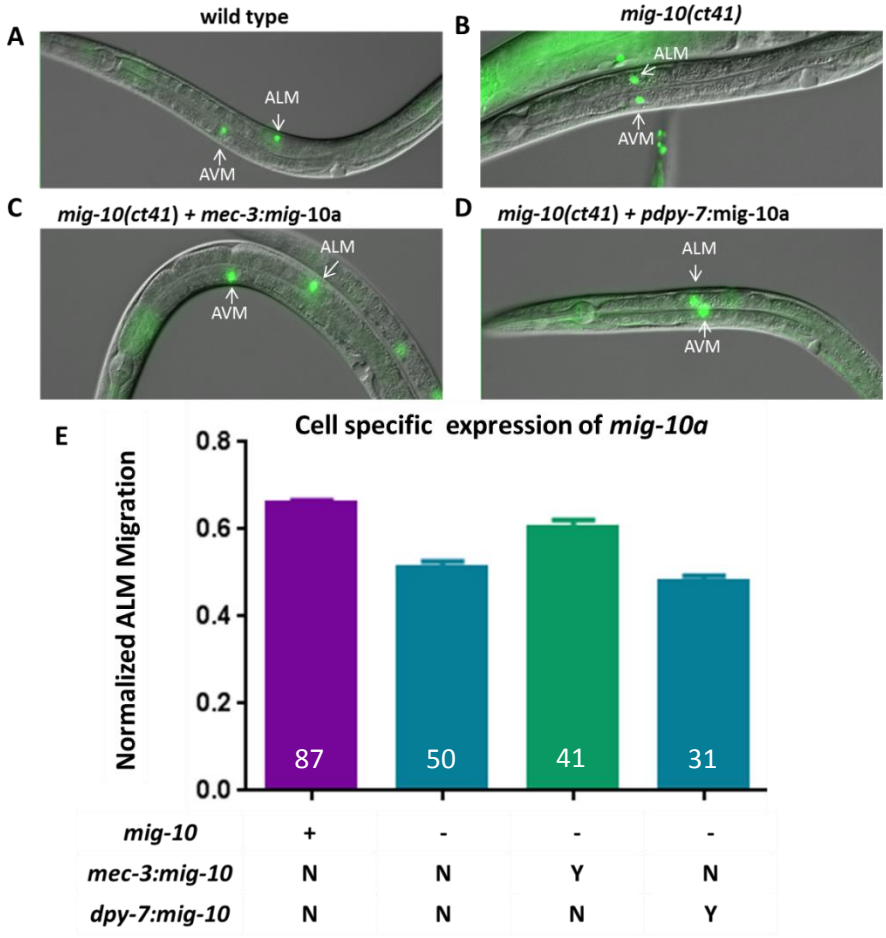

Figure 14: Rescue of *mig-10(ct41)* migration defects in the ALM. A-D, Photomicrographs of labeled strains; anterior to the left, ventral down. A. Wild type animals containing integrated *pflp-20:GFP* to visualize ALM and AVM neurons. ALM migrates posterior to AVM B. *mig-10(ct41);pflp-20:GFP* animals display truncated migration of ALM and AVM neurons. C. *mig-10(ct41)* animals with neuron specific expression of *mig-10* using *mec-3:mig-10a* transgene rescued ALM migration defects. D. *mig-10(ct41)* animals with epidermal specific expression of *mig-10* using the *dpy-7:mig-10* transgene failed to rescue ALM migration defects. C. Quantification of the normalized ALM migration. The first row is the *mig-10* genotype; next two rows are transgenes. N, no transgene present; Y, transgene present.

Rescue of neuronal migration can be seen visually by comparing images of the rescuing strain to wild type and *mig-10(ct41)* phenotypes. In wild type animals, ALM neurons migrate anterior to posterior, while AVM neurons migrate posterior to anterior. The final position of the ALM neurons is posterior to the AVM neuron (Fig 14A). However, in *mig-10(ct41)* mutants, both migrations are truncated; thus the final position of the ALM neuron is similar to the final position of the AVM neuron (Fig. 14B). ALM neurons in animals with neuron-specific expression of *mig-10* from the *mec-3::mig-10a* transgene reached a final position that was usually posterior to the AVM, similar to wild type (Fig 14C).

This result demonstrates that neuron-specific expression of *mig-10a* was able to rescue the ALM migration. In contrast, ALM neurons in animals with epidermal specific expression of *mig-10* from the *dpy-7:mig-10a* transgene failed to reach a final position posterior to the AVM neuron (Fig 14D). This suggests that epidermal specific expression of *mig-10a* cannot rescue the migration defect caused by the *mig-10(ct41)* mutation.

Quantification of the migration was performed by measuring the final position of each ALM with respect to the posterior bulb of the pharynx, which was used as a reference point. This distance was normalized by dividing by the distance from the posterior bulb of the pharynx to the vulva (See Methods). The symmetric ALML and ALMR normalized migration were averaged to obtain the normalized ALM migration shown in the Figure 14E. The *mig-10(ct41)* strain demonstrates a smaller normalized migration than wild type. The strain with neuron specific transgene *mec-3:mig-10* displayed a normalized ALM migration that fell between the mutant and the wild type strains. This result suggests that neuron specific expression of the *mig-10a* cDNA can partially rescue the ALM migration defect of *mig-10(ct41)* animals. The strain with epidermal specific transgene *dpy-7::mig-10a* showed no significant difference in normalized ALM migration from the *mig-10(ct41)* mutant strain. This result demonstrates that epidermal specific expression of *mig-10a* has no effect on the mutant phenotype. Taken together, these data suggest that MIG-10 functions cell autonomously in the ALM during migration.

ABI-1 acts cell autonomously in the ALM neurons

To determine if ABI-1 also acts cell autonomously during neuronal migration, *abi-1* was expressed specifically in the ALM neurons and the location of the ALM neurons in larval animals was quantitated. The *mec-4:abi-1*:GFP plasmid was injected into the *abi-1(tm494)* mutant strain and two independent transgenic lines (Y1 and Y2) were obtained. Normalized ALM migration was measured based on the GFP expression from the *mec-4:abi-1*:GFP transgene.

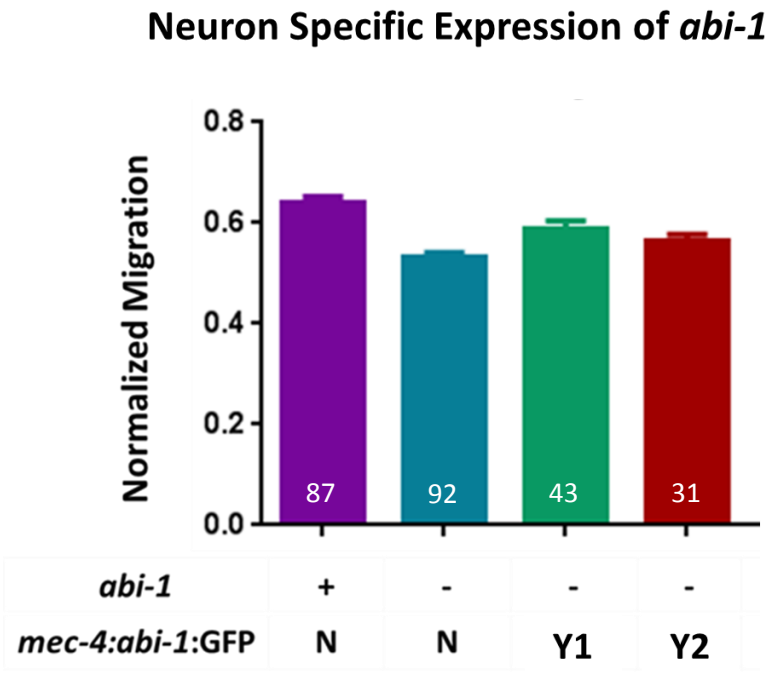

Figure 15: Neuron specific rescue of *abi-1(tm494)* migration defects. N represents no transgene present in the strain. Y1 and Y2 represent presences of the *mec-4:abi-1:GFP* in the unlabeled *abi-1(tm494)* mutant strain.

The wild type strain demonstrates the proper normalized migration of the ALM neurons (Fig. 15). Similar to the *mig-10(ct41)* mutant strain, the *abi-1(tm494)* mutant strain shows truncated ALM migration. The normalized migration of each transgenic line was significantly different from both the wild type and *abi-1(tm494)* strains. This suggests that neuron specific expression of *abi-1* can partially rescue the *abi-1(tm494)* ALM migration defect. Overall, these results suggest that cell autonomous expression of ABI-1 is sufficient to partially rescue migration defects in the ALM neurons. This is consistent with ABI-1, like MIG-10, functioning cell autonomously in the neuron to promote migration.

MIG-10 and ABI-1 act in the same pathway during neuronal migration

Thus far, it has been shown that MIG-10 and ABI-1 can each function cell autonomously in the ALM during neuronal migration. Analysis of *mig-10(ct41);abi-1(tm494)* transheterozygotes suggests that the interaction of MIG-10 and ABI-1 is important in the process of axon guidance and synaptic vesicle clustering. To investigate if MIG-10 and ABI-1 act in the same pathway *in vivo* during ALM migration, *abi-*

1(RNAi) was performed in the wild type and *mig-10(ct41)* mutant background, and normalized ALM migration was measured. The normalized migration of the ALM in a wild type strain fed an empty vector RNAi control, a *mig-10(ct41)* mutant strain and an *abi-1(tm494)* mutant strain were quantitated to use for comparison. Wild type animals fed *abi-1(RNAi)* exhibited significantly truncated ALM migration compared to the wild type strain fed the empty vector RNAi (Fig. 16). The truncation of ALM migration suggests that *abi-1(RNAi)* was effective in targeting the *abi-1* transcript. However, the migration defect from *abi-1(RNAi)* is less severe than the *abi-1(tm494)* mutant. *mig-10(ct41)* animals fed *abi-1(RNAi)* showed normalized migration similar to the *mig-10(ct41)* mutant. If these two proteins were acting in parallel pathways, knocking down *abi-1* expression in a *mig-10(ct41)* mutant background would produce an enhanced defect compared to the *mig-10(ct41)* mutant alone. These data showed no enhancement of the migration defects, suggesting that MIG-10 and ABI-1 promote migration by acting in the same pathway. Taken together, these results are consistent with the model that MIG-10 and ABI-1 are both acting in the same pathway in the neuron to promote migration.

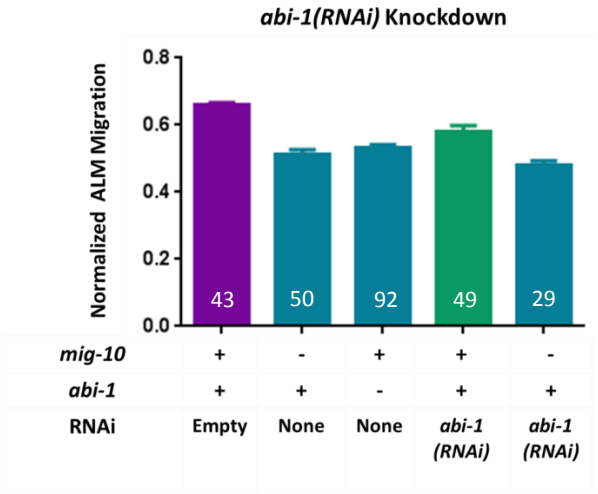

Figure 16: *abi-1(RNAi)* fed to the wild type and *mig-10(ct41)* mutant strains. Empty, empty vector *RNAi*; None, no *RNAi*. *abi-1(RNAi)* in the wild type strain produced truncated migration of the ALM. *abi-1(RNAi)* in the *mig-10(ct41)* strain displayed no enhancement of the migration defect compared to the *mig-10(ct41)* mutant or *abi-1(RNAi).*

MIG-10 and ABI-1 neuron specific feeding produced no ALM migration defect

To support the conclusion that MIG-10 and ABI-1 acts autonomously in the ALM, tissue specific knockdown of *mig-10* and *abi-1* was performed by feeding RNAi. In *C. elegans,* RNAi is systemic, meaning that the knockdown of the desired transcript occurs in every cell of the animal. However, this knockdown is inefficient in some cell types, such as the neurons. It has been shown that the SID-1 transporter is essential for double stranded RNA to enter the cell. Neurons express the SID-1 transporter at lower levels than other cells, which explains the inefficiency of RNAi in this cell type (Calixo et al., 2010). Strains have been developed that contain a null mutation in the *sid-1* gene, causing RNAi to be non-functional in all cell types. Tissue specific expression of the *sid-1* cDNA from a transgene allows the double stranded RNA to be taken up only by specific cell types. A strain, TU3595, containing pan neuronal expression of *sid-1* from a transgene in a *sid-1* mutant background, was obtained to allow for neuron specific uptake of RNAi. To determine if MIG-10 or ABI-1 is necessary in the neuron for proper migration, RNAi knockdown of each transcript was performed in the wild type and TU3595 strains.

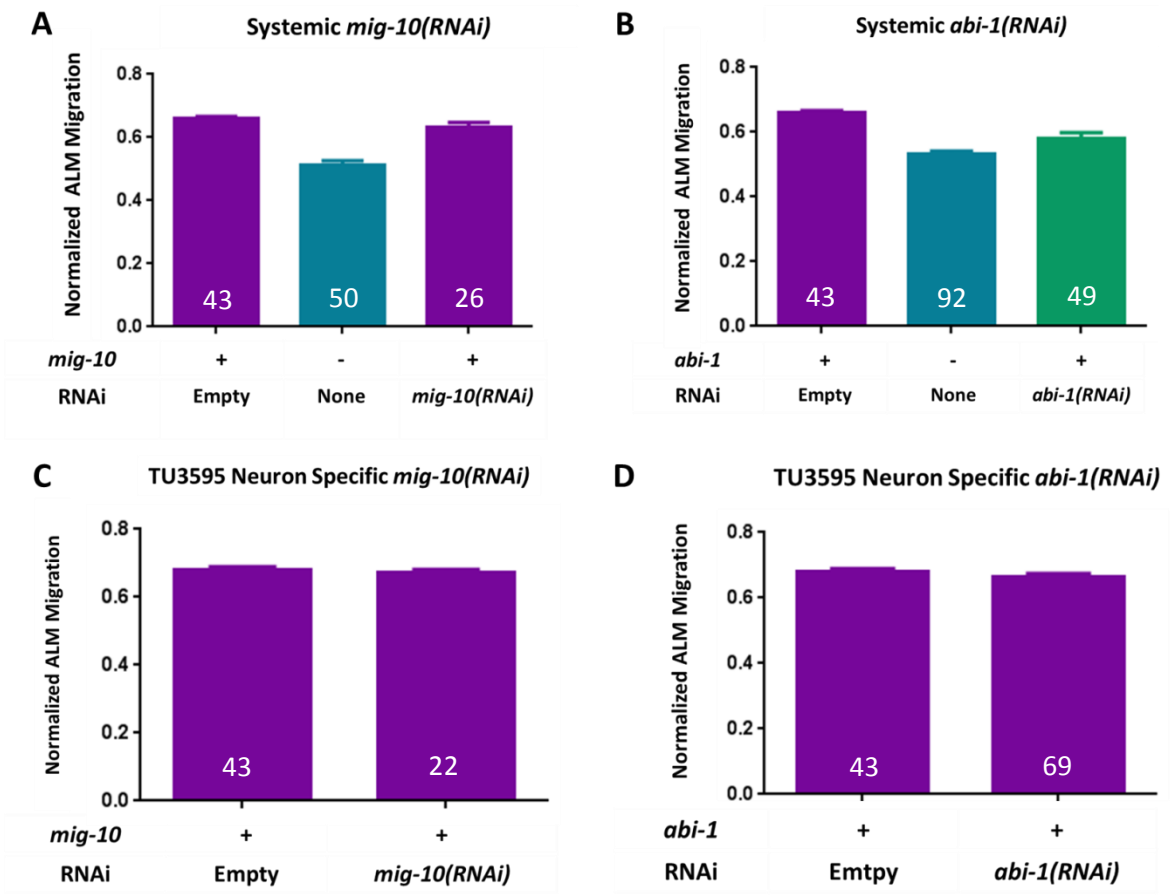

Figure 17: Tissue specific knockdown using *mig-10(RNAi)* and *abi-1(RNAi)*. A. *mig-10(RNAi)* in a wild type background produces no effect on normalized ALM migration. B. *abi-1(RNAi)* in a wild type background show truncated normalized ALM migration compared to wild type animals. C. *mig-10(RNAi)* in the neuron specific RNAi strain, TU3595, showed no migration defect of the ALM. *abi-1(RNAi)* in the neuron specific RNAi strain, TU3595, showed no migration defect of the ALM.

Animals fed empty vector RNAi were quantitated as a control and these animals displayed no migration defects. The normalized migration of wild type animals fed *mig-10(RNAi)* was compared to animals fed an empty vector RNAi and the *mig-10(ct41)* mutant strain. *mig-10(RNAi)* demonstrated no significant difference in normalized migration of *mig-10(RNAi)* compared to the control animals (Fig. 17A).

The normalized migration of wild type animals fed *abi-1(RNAi)* was compared to animals fed empty vector RNAi and *abi-1(tm494)* mutant animals. The migration defect of wild type animals fed *abi-1(RNAi)* was less severe than the defect displayed by *abi-1(tm494)* animals. However, *abi-1(RNAi)*

showed significantly smaller normalized ALM migration than the control animals. These results suggest that *abi-1(RNAi)* knocked down the *abi-1* transcript in the wild type strain (Fig. 17B).

To address cell autonomy, *mig-10*(RNAi) was fed to the TU3595 strain which allows for neuron specific uptake of RNAi. The *mig-10(RNAi)* produced no migration defect in the TU3595 background, showing no statistical difference in migration from the animals fed an empty vector control (Fig. 17C). The *abi-1(RNAi)* also produced no migration defect, displaying no statistical difference from the animals fed an empty vector control (Fig. 17D).

As these experiments were performed simultaneously, the strategy of RNAi feeding and the *abi-1(RNAi)* strain were demonstrated to be effective in the wild type strain causing an ALM migration defect but not in the TU3595 strain. Therefore, conclusions about cell autonomy were not possible as neither the *mig-10(RNAi)* nor the *abi-1(RNAi)* experiment showed any effect on the TU3595 strain.

Transgenic knockdown of *mig-10* showed no ALM migration defect

Due to the inability of *mig-10*(RNAi) to produce migration defect in either the wild type or the TU3595 neuron specific RNAi strain, a transgenic approach was undertaken. To support the conclusion that *mig-10* acts cell autonomously, 100bp sense and antisense fragments of a *mig-10* exon were obtained through directional PCR. Each fragment was cloned into a vector containing the *mec-4* promoter by Rebekah Cocks (See methods). The *mec-4:mig-10* sense and *mec-4:mig-10* antisense plasmids were injected together into wild type animals containing an integrated *pflp-20*:GFP at equal concentration along with the *unc-122*:RFP co-injection marker. A transgenic line containing *mig-10* sense and antisense fragments was produced.

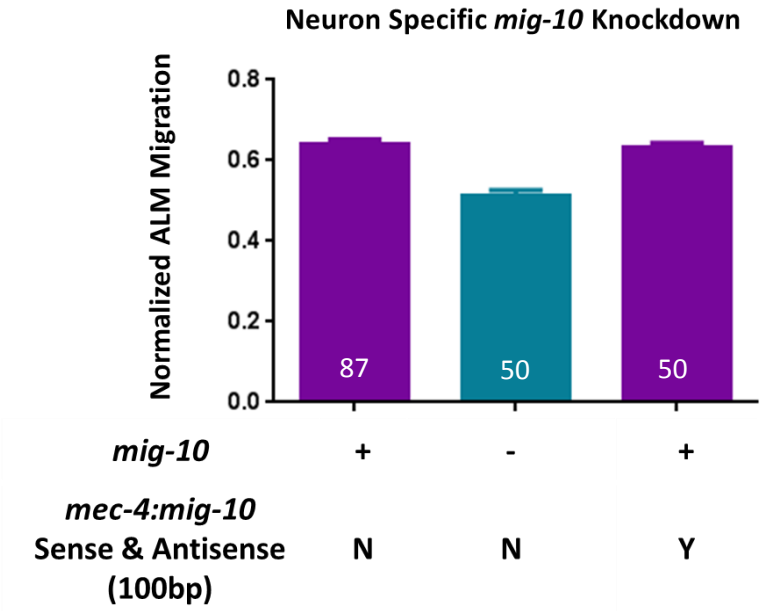

Figure 18: Neuron specific knockdown of *mig-10* using 100bp sense and antisense fragments of *mig-10*. Injection of *mec-4:mig-10* sense and *mec-4:mig-10* antisense together produced no ALM migration defect.

The normalized migration of the wild type and *mig-10(ct41)* strains was compared to the transgenic line with neuron specific expression of the *mig-10* sense and antisense fragments. The strain containing the *mec-4:mig-10* sense and antisense fragments together showed no statistical difference compared to the wild type strain (Fig. 18). This may suggest that the strategy of using short fragments of the *mig-10* gene was ineffective at knocking down the *mig-10* transcript. Alternatively, it may suggest that MIG-10 is produced very early and/or in high quantities during development. The *mec-4* promoter used to express the *mig-10* sense and antisense fragments may be expressed later or too weakly during development. Therefore, the RNAi cannot knock down enough of the transcript to produce a migration defect in the ALM because there is already enough protein present to promote migration in the neuron.

abi-1 antisense displays no ALM migration defect

Due to the inability of the *mig-10* sense and antisense fragments to produce a migration defect, a new strategy for knockdown was performed. Neuron specific knockdown of *abi-1* was performed by injection of the *mec-4:abi-1* antisense construct and *unc-122*:RFP co-injection marker into wild type

animals at two different concentrations 50ng/µl and 100ng/µl. Additionally, to investigate any non-autonomous function ABI-1, a *dlg-1:abi-1* antisense construct was designed to produce *abi-1* antisense in the epidermal cells underlying the ALM neuron. This *dlg-1:abi-1* antisense plasmid was injected into wild type animals at 100ng/µl and two transgenic lines were established.

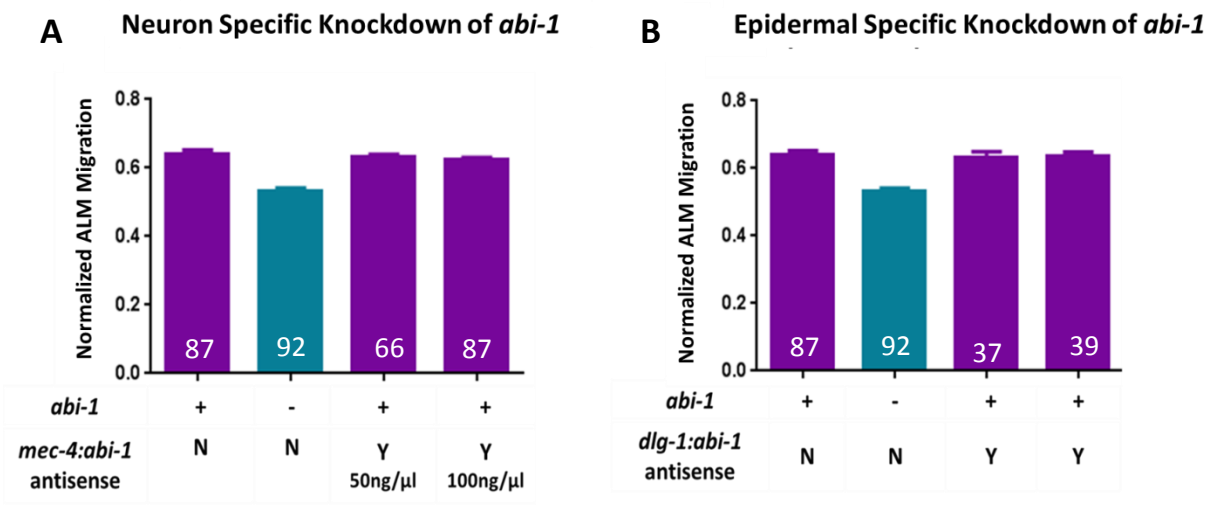

Figure 19: Tissue specific knockdown of *abi-1*. A. Neuron specific knockdown of *abi-1* from *mec-4:abi-1* antisense displayed no ALM migration defect. B. Epidermal specific knockdown of *abi-1* from *dlg-1:abi-1* antisense displayed no ALM migration defect.

The transgenic strains containing 50ng/µl and 100ng/µl of *mec-4:abi-1* antisense was compared to the wild type and *abi-1(tm494)* mutant strains. The normalized migration of neither transgenic strain expressing *mec-4:abi-1* antisense showed no statistical difference compared to the normalized migration of the wild type strain (Fig. 19A). This result may indicate that the strategy of knockdown of *abi-1* using the *mec-4:abi-1* antisense transgene is ineffective.

The normalized migration of two independent lines expressing *dlg-1:abi-1* antisense was compared to wild type and *abi-1(tm494)* mutant strains. Each of the independent lines injected at 100ng/µl displayed no ALM migration defects and the normalized migration was not significantly different from the wild type strain (Fig. 19B). Taken together, these results suggest that using the antisense strand of *abi-1* to knock down the endogenous *abi-1* transcript was an ineffective strategy.

This could happen if ABI-1 is produced very early and/or in high quantities during development. The *mec-4* promoter may be expressed too late or weakly in development to achieve effective knockdown of the protein. Therefore, knockdown of the transcript, would fail to produce a migration defect in the ALM because there is already enough protein present for the neuron to migrate. However, the *mec-4* promoter may be sufficiently early/strong to produce enough of the protein to partially rescue.

A final strategy was attempted to elucidate the effects of neuron specific knockdown of *abi-1* on ALM migration. The *mec-4:abi-1*:GFP and *mec-4:abi-1* antisense plasmids were injected into wild type animals together at equal concentrations with the *unc-122*:RFP co-injection marker. It was hypothesized that the sense and antisense strands of *abi-1* would be transcribed in the neuron. Once transcribed, the sense and antisense strands would create dsRNA and this may produce a more efficient knockdown than the antisense alone.

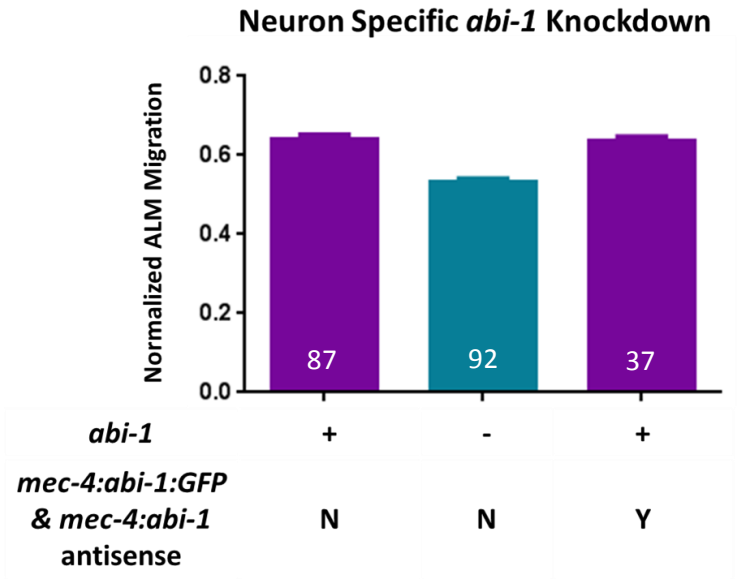

Figure 20: Neuron specific knockdown of *abi-1*. *mec-4:abi-1*:GFP and *mec-4:abi-1* antisense plasmids were injected together into wild type animals. No ALM migration defects were detected in this transgenic line.

The normalized migration of transgenic animals expressing both *mec-4:abi-1:*GFP and *mec-4:abi-1* antisense transgenes was compared to the wild type and *abi-1(tm494)* mutant strains. The transgenic

strain with neuron specific expression of *mec-4:abi-1*:GFP and *mec-4:abi-1* antisense displayed no ALM migration defects and was not statistically different from the wild type strain (Fig. 20). Therefore, this strategy was not effective in providing any further insight into whether ABI-1 acts cell autonomously in the ALM. Because none of the knockdown strategies had any effect on either *abi-1* or *mig-10* in either the neuron or the underlying epidermal cells, it cannot be concluded if these proteins are functioning cell autonomously by knockdown.

Effect of cell specific expression of *mig-10* and *abi-1* on the AVM

To determine whether *mig-10* acts cell autonomously in the AVM neuron, *mig-10* was expressed in the AVM neuron or in the underlying epidermis and the position of the AVM neuron was quantified. The AVM neuron migrates in the opposite direction of the ALM, from the posterior of the animal to the anterior. In the same experiments used to quantitate the normalized ALM migration, the normalized AVM migration was also quantitated in the same animals. In the first set of experiments discussed previously, the *mig-10(ct41)* mutant strain was injected with either *mec-3:mig-10a* to allow for neuronal specific expression of *mig-10* , or *dpy-7:mig-10a* to allow for epidermal specific expression. Additionally, to determine if *abi-1* acts cell autonomously neuron specific expression of *abi-1* was also performed. *mec-4:abi-1*:GFP was injected into *abi-1(tm494)* mutant animals. The normalized AVM migration of the two transgenic strains Y1 and Y2 was measured based on the GFP expression from the *mec-4:abi-1:*GFP transgene.

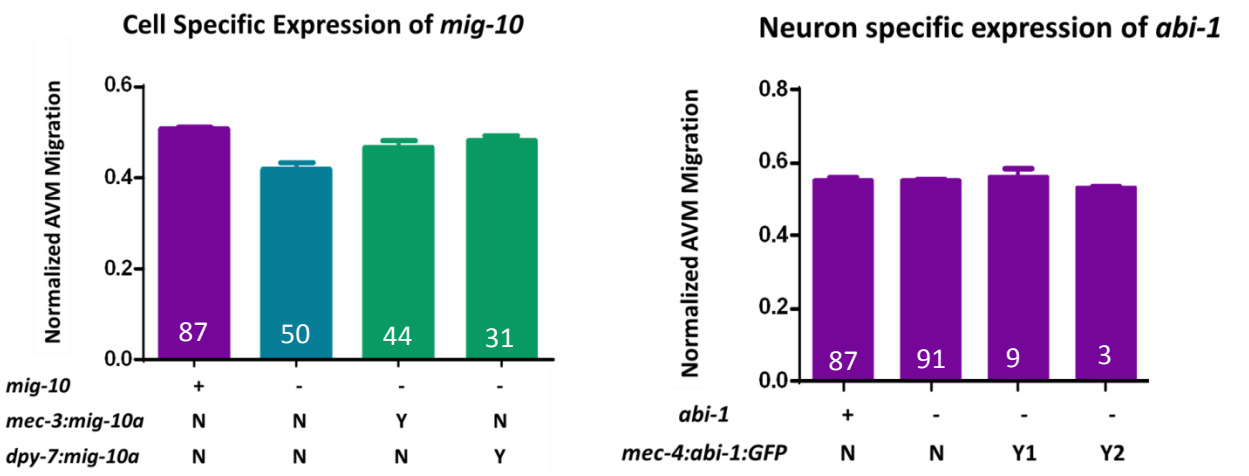

Figure 21: Cell specific expression of *mig-10* and *abi-1*. A. Both neuron specific and epidermal specific expression of *mig-10* can partially rescue *mig-10(ct41)* AVM migration defects. B. Neuron specific expression of *abi-1* shows no difference in AVM migration for wild type or *abi-1(tm494)* mutant strains. N, no transgene present; Y, transgene present.

mig-10(ct41) mutant animals containing the *mec-3:mig-10a* transgene displayed a normalized migration that fell between the wild type and *mig-10(ct41)* mutant strains (Fig. 21A). This result suggests that neuron specific expression of *mig-10a* cDNA can partially rescue the AVM migration defect of *mig-10(ct41)* animals. *mig-10(ct41)* mutant animals containing the *dpy-7:mig-10a* transgene also displayed a normalized migration between the wild type and *mig-10(ct41)* mutant strain (Fig. 21A). This result suggests that epidermal specific expression of mig-10a is also capable of rescuing the AVM migration defect of *mig-10(ct41)* animals. Taken together these results may suggest some non-autonomous function of *mig-10* in the AVM neurons.

The *abi-1(tm494)* mutant displayed no migration defects in the AVM, however, this may be because *abi-1(tm494)* is a weak mutant strain. The *abi-1(tm494)* mutant animals containing the *mec-4:abi-1*:GFP transgene displayed a normalized migration that was not significantly different than the wild type or the *abi-1(tm494)* mutant strain (Fig. 21B). These results suggest that the *abi-1(tm494)* mutant strain does not display an AVM migration defect and it is possible that ABI-1 is not functioning in the AVM during migration.

Tissue Specific knockdown of *mig-10* and *abi-1* in the AVM

To support the hypothesis that *mig-10* may have some non-autonomous function and *abi-1* does not function in the AVM during migration, normalized migration of the AVM was quantitated from the tissue specific knockdown of *mig-10* and *abi-1* performed by RNAi feeding. Recall, RNAi knockdown in the wild type strain causes systemic knockdown of the target transcript while the TU3595 strain only allows for neuron specific uptake of the dsRNA. The wild type and TU3595 animals were fed *mig-10(RNAi)* and *abi-1(RNAi)* to determine if these proteins are functioning in the AVM neuron during migration. Again, the normalized AVM migration was quantitated during the same experiment and within the same animals that the normalized ALM migration was quantitated.

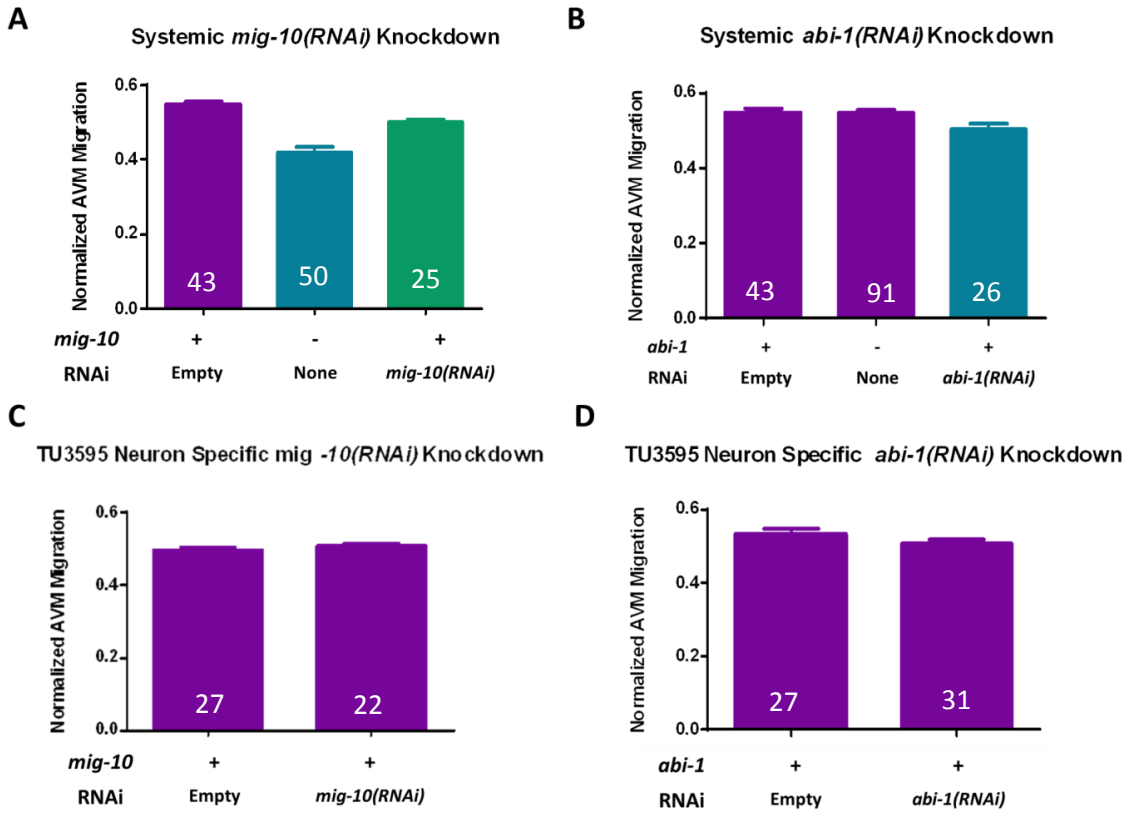

Figure 22: Tissue specific knockdown using *mig-10(RNAi)* and *abi-1(RNAi)*. A. *mig-10(RNAi)* in a wild type background showed truncated normalized AVM migration compared to wild type animals. B. *abi-1(RNAi)* in a wild type background show truncated normalized AVM migration compared to wild type animals. C. *mig-10(RNAi)* in the neuron specific RNAi strain, TU3595, showed no migration defect of the ALM. *abi-1(RNAi)* in the neuron specific RNAi strain, TU3595, showed no migration defect of the ALM.

Animals fed empty vector RNAi were quantitated as a control and these animals displayed no AVM migration defects. The normalized migration of wild type animals fed *mig-10(RNAi)* was compared to animals fed an empty vector RNAi and the *mig-10(ct41)* mutant strain. *mig-10(RNAi)* demonstrated a smaller normalized migration of *mig-10(RNAi)* compared to the control animals (Fig. 22A) This suggests that the *mig-10(RNAi)* is knocking down some of the mig-10 transcript to cause the AVM migration defect.

The normalized migration of wild type animals fed *abi-1(RNAi)* was compared to animals fed empty vector RNAi and *abi-1(tm494)* mutant animals. *abi-1(RNAi)* also showed a smaller normalized AVM migration than the control animals (Fig. 22B) These results suggest that the *abi-1(tm494)* is a weak mutant in and the effects of *abi*-1*(RNAi)* allow a stronger defect in AVM migration to be visualized.

The *mig-10(RNAi)* produced no migration defect in the TU3595 background and showed no statistical difference in normalized migration from the control animals (Fig. 22C). Similar to the *mig-10(RNAi)*, the *abi-1(RNAi)* also produced no AVM migration defect, displaying no statistical difference from the TU3595 control animals (Fig. 22D). These results suggest that both *mig-10* and *abi-1* may possess some non-autonomous function during AVM migration. However, the TU3595 strain does not display a migration defect from either strain of RNAi. Without a positive control, it cannot be determined if this strain successfully uptakes RNAi in the neurons.

Effect of neuron specific knockdown of *abi-1* in the AVM

To further investigate cell autonomy of *mig-10* and *abi-1* during AVM migration, the effect of knockdown of *abi-1* on the AVM, using a transgenic strategy, was quantitated in the same animals that the normalized ALM migration was quantitated. Neuron specific knockdown of *abi-1* was performed by injection of *mec-4:abi-1* antisense and by injection of both *mec-4:abi-1* antisense and *mec-4:abi-1*:GFP

into the wild type strain. Epidermal specific knockdown of *abi-1* was performed by injection of *dlg-1:abi-1* antisense into the wild type strain.

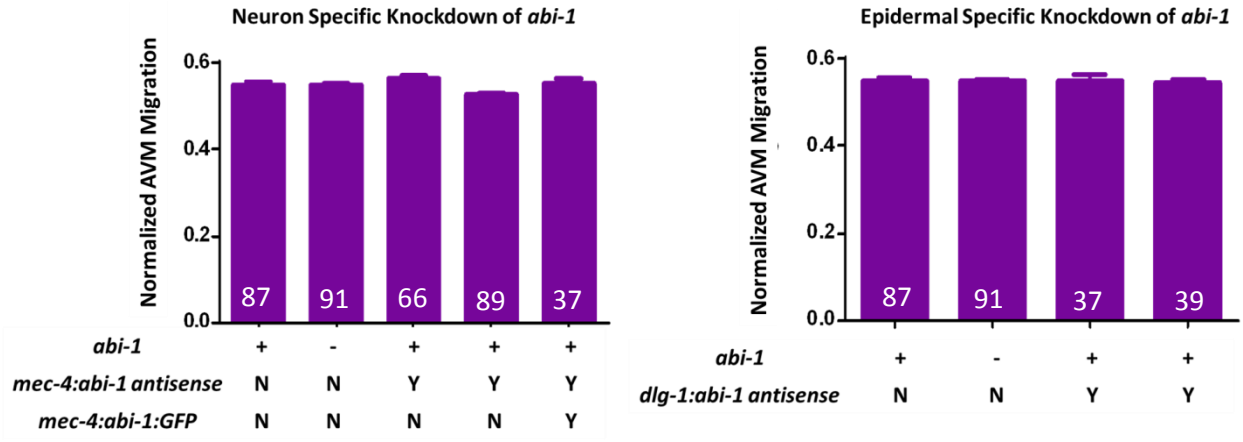

Figure 23: Tissue specific knockdown *abi-1*. A. Neuron specific knockdown of *abi-1* from *mec-4:abi-1* antisense displayed no AVM migration defect. B. Epidermal specific knockdown of *abi-1* from *dlg-1:abi-1* antisense displayed no AVM migration defect.

Neuron specific expression of the *abi-1* antisense from the *mec-4:abi-1* transgene demonstrated no statistical difference in AVM migration compared to the wild type or *abi-1(tm494)* weak mutant strain (Fig. 23A) . The knockdown of the *abi-1* transcript by co-injection of *mec-4:abi-1*:GFP and *mec-4:abi-1* antisense also displayed no migration defect in the AVM. Additionally, epidermal specific expression of *abi-1* from the *dlg-1:abi-1* antisense transgenes showed no significant difference in AVM migration compared to the wild type or *abi-1(tm494)* strains. These results suggest that *abi-1* is not functioning during the process of AVM migration or that the strategy of using *abi-1* antisense to knock down expression of *abi-1* is not effective.

Discussion

Cellular migration is an essential process for establishing neuronal connections during development. During migration the neuron must respond to guidance cues in the environment and transduce those signals into cytoskeletal re-arrangements at the leading edge. The cytoplasmic adaptor proteins MIG-10 and ABI-1 have been shown to participate in the process of axon guidance and excretory cell outgrowth. In axon guidance, the upstream guidance cue, UNC-6, has been shown to bind to the UNC-40 receptor (Xu et al., 2012). Downstream of these molecule, it has been shown that MIG-10 and ABI-1 act together in axon guidance. However, the pathway in neuronal migration is much less defined. *mig-10(ct41)* and *abi-1(tm494)* mutants display similar defects in neuronal migration, consistent with the model in axon guidance, but it had not been shown that these two genes are acting cell autonomously and in the same pathway during neuronal migration. The results of this study demonstrate that neuron specific expression of *mig-10* or *abi-1* is sufficient to partially rescue the ALM migration defect of *mig-10(ct41)* or *abi-1(tm494)* mutant animals, respectively. In addition, recent work has shown that expression of *mig-10* from the *mec-4* promoter can completely rescue migration in *mig-10(ct41)* mutants (Zhang and Ryder, unpublished results). Furthermore, the current work demonstrated no enhancement of the ALM migration defect displayed by *mig-10(ct41)* animals when fed *abi-1(RNAi)*. These results support the model demonstrating that *mig-10* and *abi-1* functioning cell autonomously in the same signaling pathway during ALM migration.

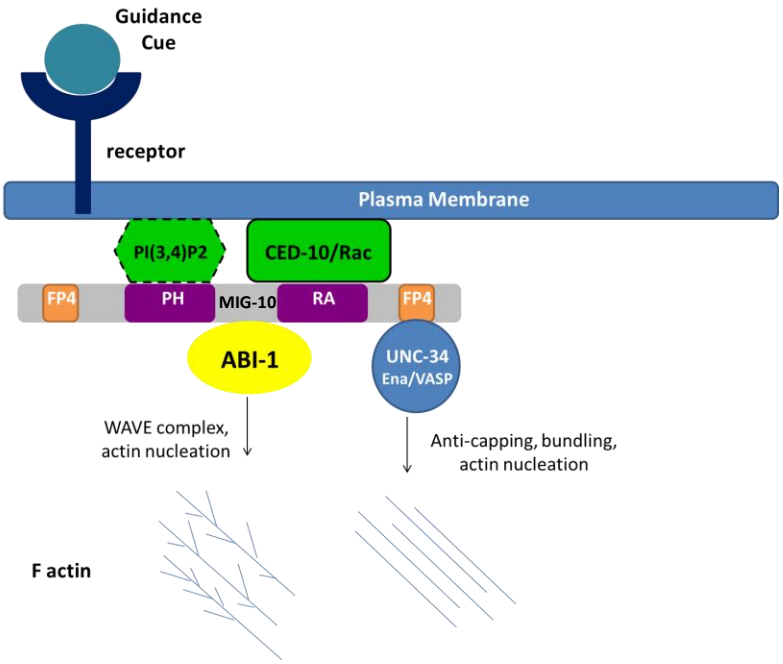

Figure 24: Proposed model for ALM migration. Unlike axon guidance, the guidance cue and receptor have not been defined in neuronal migration. This work has demonstrated that MIG-10 and ABI-1 may function autonomously in the same pathway to promote ALM migration.

AVM migration may function by a different mechanism than ALM migration

The AVM neuron is produced by the differentiation of the QR neuroblast. The QR neuroblasts are born approximately one hour before hatching and migrate toward the anterior of the animal. The AVM, the descendant of this neuroblast, continues migrating toward the anterior of the animal to reach its final position in the animal by the end of the first larval stage (Salser & Kenyon, 1992). The migration from posterior to anterior and the migration of its precursor cell are two of the major differences from the phenotype of ALM migration. The *mig-10(ct41)* mutant displays truncated migration of the AVM, however, partial rescue of migration was achieved through both neuron specific and epidermal specific expression of *mig-10.* In contrast, partial rescue was only achieved by neuron specific expression in the ALM. Further investigation of non-autonomous function of *mig-10* in AVM migration should be performed.

The *abi-1(tm494)* mutant does not produce an AVM migration defect. As the *abi-1(tm494)* mutant is a weak mutant, the effect of cell specific rescue and knockdown was performed to determine if there is a role of ABI-1 during AVM migration. There was no effect of neuron specific expression of *abi-1* on AVM migration. Knockdown of *abi-1* was also ineffective in all strategies; therefore this work could not conclude anything about the role of ABI-1 in AVM migration. Due to the differences in the migration phenotype, it is possible that the ALM and AVM neurons migrate using a different mechanism.

Investigation of non-autonomous function of MIG-10 or ABI-1 by feeding RNAi

Because there was some evidence the *mig-10* and *abi-1* may act in underlying epidermal cells during outgrowth of the excretory cell (Manser, 1997; McShea, 2013), efforts were made to determine whether there might be some non-autonomous function for *mig-10* or *abi-1* during neuronal migration. Previous investigators have developed strains for performing tissue specific RNAi knockdown. The SID-1 transporter, which uptakes dsRNA into the cell, is necessary for function of the RNAi mechanism. The TU3595 strain used in these RNAi knockdown experiments contains a *sid-1* mutant background with neuron specific expression of *sid-1* from the pan neuronal promoter *unc-119*. This strain also contains a *lin-15b* mutation which has been shown to enhance the effects of RNAi. In this study *mig-10(RNAi)* or *abi-1(RNAi)* failed to produce migration defects in the ALM using the neuron specific TU3595 strain. However, the *abi-1(RNAi)* in the wild type strain displayed a smaller normalized ALM migration than the wild type strain demonstrating the strategy was successful in knocking down the *abi-1* transcript in the wild type strain (Fig. 25).

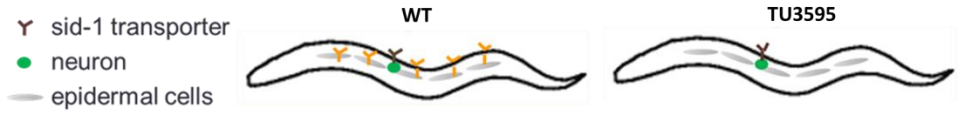

	WILD TYPE	TU3595 Neuron Specific Strain
Empty vector (RNAi)	No migration defect	No migration defect
***mig-10* (RNAi)**	No migration defect	No migration defect
***abi-1* (RNAi)**	**Truncated migration**	No migration defect

Figure 25: Summarized results of feeding RNAi in the ALM. In the wild type strain only *abi-1(RNAi)* produced a migration defect. In the TU3595 neuron specific RNAi strain neither *mig-10(RNAi)* nor *abi-1(RNAi)* produced a migration defect.

Given that the *abi-1(RNAi)* is effective in the wild type strain, where neuronal uptake of dsRNA is inefficient, it is possible that there is some non-autonomous function of ABI-1 in ALM migration. However, since neither *mig-10(RNAi)* nor *abi-1(RNAi)* produced an effect in the neuron specific strain, it is possible that the strain is not taking up the dsRNA properly into the neurons. Although the *mig-10(RNAi)* plasmid was sequenced, it is also possible that it is not functioning effectively to create dsRNA, since it had no effect in either strain. Thus, no conclusions about cell autonomy could be made from this work. In future work, the RNAi vector targeting a gene previously shown to work effectively in the TU3595 strain could be ordered and incorporated into the experimental design.

Transgenic knockdown of MIG-10 or ABI-1

A transition to a transgenic strategy for knock down was made as it has been shown to be more effective in knockdown of specific cell types. Using this strategy to specifically knockdown neuronal genes was hypothesized to be more effective as the inefficient process of dsRNAi uptake by the neuron would be eliminated. As *mec-4:mig10a* had demonstrated complete rescue of ALM migration in other work, neuron specific knockdown of *mig-10* was attempted initially as a method of validating the knockdown strategy. However neuron specific knockdown of *mig-10* from transgenes containing *mec-4:mig-10a* (100bp) sense and *mec-4:mig-10a* (100bp) antisense did not produce a migration defect similar to the *mig-10(ct41)* mutant. Validation of this strategy would need to be done to conclude that

mig-10 is not functioning cell autonomously in the neuron. This could be done by performing knockdown using this strategy on of a gene known to act in the neuron.

This study was more interested in the cell autonomy of *abi-1* due to the stronger evidence already available for *mig-10* autonomous function. Therefore neuronal specific knockdown of *abi-1* and epidermal specific knockdown of *abi-1* was attempted using the full length antisense strand of *abi-1*, a strategy used by other investigations. It was hypothesized that the antisense strand of *abi-1* would be produced in the specific cell type and bind to the exogenous full length copy of *abi-1* triggering the RNAi mechanism. However, ALM or AVM migration defects were not seen in animals expressing either the neuron specific or epidermal specific cell type. As these are the most likely cell types involved in migration, this strategy was regarded as ineffective at knocking down the *abi-1* transcript. This may be due to some inefficiency of the *abi-1* antisense produced from by the *mec-4:abi-1* antisense to bind to the endogenous copy. Following up on that hypothesis, both the *mec-4:abi-1* antisense and *mec-4:abi-1:*GFP were co-injected into wild type animals. Expressing both transgenes may promote more the binding of the sense and antisense copies and therefore may trigger the mechanism of RNAi knockdown more effectively. However, no ALM or AVM migration defect was produced by neuron specific expression of both the sense and antisense copies of *abi-1*. Both of these strategies should be validated more closely to determine if it is capable of knocking down a transcript specifically functioning in the neuron (Table 2).

Cell Type Targeted	Transcript Targeted	Strategy Used	Result
Neurons	*mig-10*	100bp sense and antisense fragments of *mig-10* cDNA	**No ALM or AVM migration defect**
Neurons	*abi-1*	Antisense strand of *abi-1*	**No ALM or AVM migration defect**
Epidermal Cells	*abi-1*	Antisense strand of *abi-1*	**No ALM or AVM migration defect**
Neurons	*abi-1*	Full length sense and antisense strand of *abi-1*	**No ALM or AVM migration defect**

Table 2: Summary of transgenic knockdown results. Four strategies were attempted; No strategy produced a migration defect in the ALM or AVM

Future work performing neuron specific knockdown of *mig-10* and *abi-1*

The common element of that all the transgenic neuron specific knockdown strategies incorporated is the *mec-4* promoter. It may be possible that that the *mec-4* promoter is expressed early enough to drive enough protein production in the mutant background for proper migration to occur. However, the promoter may not turn on early enough or strong enough to knock down enough of the transcripts necessary to produce a migration defect. *mec-4* is expressed before the ALM neurons begin migrating. It was determined that this promoter would be effective because complete rescue was achieved by expression of *mec-4:mig-10a*. The results demonstrating partial rescue from neuron specific expression of each gene suggests that when the protein is produced before migration begins, then it can function to promote migration. However, if the antisense or RNAi is only being produced a short time before migration, it may not act quickly enough to knock down a sufficient amount of transcript. This would lead to no migration defect being displayed in these animals. Additionally, if the protein has already been made before the *mec-4* promoter begins expressing the antisense, then knocking down the transcript will not inhibit the protein from performing its function and migration would progress normally.

Future work is in progress to express all of the plasmids used in the prior strategies under control of a new neuron specific promoter. The *unc-86* promoter will be used as it is expressed earlier during development than the *mec-4* promoter. The *unc-86* promoter is expressed at approximately 150 minutes after fertilization (26 cell stage) when gastrulation begins, which is much earlier than ALM migration which begins approximately 390 minutes after fertilization which is after twitching (Bucher & Seydoux, 1994, von Ehrenstein & Schierenberg, 1980, Wood, 1988, and Sulston et al., 1983).

The *unc-86* promoter has already been cloned into all of the plasmids that originally contained the *mec-4* promoter. These plasmids should be injected into wild type animals at the same concentrations that the *mec-4* plasmids were injected at to provide an accurate comparison of the two promoters. Also for comparison, rescue of *abi-1(tm494)* migration defects should be investigated using the *unc-86* promoter.

Future work to support the model that MIG-10 localizes ABI-1

Another area needing further investigation is the localization of ABI-1 in the migrating ALM neuron. In mammalian cells, ABI-1 has been shown to localize to the leading edge of migrating cells. However, *abi-1*:GFP has not been able to be visualized in the HSN neuron during migration in *C. elegans*. (Quinn 2012) The model supported by this work hypothesizes that MIG-10 is recruited to the leading edge of the neuron due to guidance cue binding. Once MIG-10 has been recruited to the leading edge, it can then localize ABI-1 to the leading edge which allows for cytoskeletal reorganization to occur. If this model is supported, the localization of ABI-1 should be disrupted if the MIG-10 protein is absent. Therefore, *abi-1*:gfp expression should be examined in wild type and *mig-10(ct41)* mutant embryos during the time of ALM migration. This investigation has some challenges. ALM migration is later than other neurons such as the CAN neuron and therefore the ALMs are migrating while the embryo begins twitching. The embryo moves rapidly during this time and therefore examining expression at this stage may be difficult. However, differences in localization could be examined slightly before twitching begins

and attempted after twitching as well. This strategy has been preliminarily investigated using a wild type strain injected with *mec-4:abi-1*:GFP. This strain also contains *pflp-20*:GFP which labels a subset of mechanosensory neurons and therefore the expression pattern is not meaningful. However, the embryo prep allowed for visualization of the ALM neurons suggesting a promising strategy for investigating localization. This investigation is currently being performed by crossing the *mec-4:abi-1*:GFP array into the *mig-10(ct41)* mutant background. Once a strain containing the array in the *mig-10(ct41)* background has been established, the *abi-1*:GFP expression can be examined in the embryos and compared to wild type expression of *abi-1*:GFP. It is hypothesized that *abi-1*:gfp would be localized to the leading edge of the neuron in wild type embryos. However, the *abi-1*:gfp would be distributed throughout neuron in the *mig-10(ct41)* null mutant as there is no MIG-10 protein for ABI-1 to bind and become localized. This evidence would confirm that MIG-10 is localizing ABI-1 to the leading edge in vivo to promote proper migration of the ALM neurons.

Future work to fully characterize role of MIG-10, ABI-1 & UNC-34 in migration

Further investigation can be performed to determine if UNC-34 and ABI-1 represent all of the MIG-10 effectors and establish whether MIG-10 is the only protein capable of localizing members of the actin polymerization machinery. It has been demonstrated that UNC-34 is not responsible for potentiating the entire outgrowth promoting activity of MIG-10. ABI-1 has been shown to be another effector of MIG-10 allowing for changes in actin cytoskeleton. To further characterize the roles of MIG-10, ABI-1 and UNC-34 during this process, neuron specific knockdown of the *abi-1* transcript in an *unc-34* null mutant strain should be performed. If there is no difference in ALM migration when compared to the *mig-10* null mutant then the result is consistent with only the MIG-10 protein being able to localize ABI-1 and UNC-34. If the ALM migration defect of *abi-1* knockdown in the *unc-34* null mutant background is less severe than *mig-10(ct41)* null mutant than MIG-10 must have other effectors capable of promoting migration. Finally, if the migration defect is more severe than the *mig-10(ct41)* null mutant then there is something

else that is capable of localization or localization is not absolutely required for migration. This experiment would fully characterize the role for each of these cytoplasmic adaptor proteins during the process of neuronal migration.

References

Altun, Z. F. a. H., D.H. . (2011.). Nervous system, general description. *In WormAtlas.* doi: 10.3908/wormatlas.1.18

Applewhite, D. A., Barzik, M., Kojima, S., Svitkina, T. M., Gertler, F. B., & Borisy, G. G. (2007). Ena/VASP proteins have an anti-capping independent function in filopodia formation. *Mol Biol Cell, 18*(7), 2579-2591. doi: 10.1091/mbc.E06-11-0990

Barzik, M., Kotova, T. I., Higgs, H. N., Hazelwood, L., Hanein, D., Gertler, F. B., & Schafer, D. A. (2005). Ena/VASP proteins enhance actin polymerization in the presence of barbed end capping proteins. *J Biol Chem, 280*(31), 28653-28662. doi: 10.1074/jbc.M503957200

Bear, J. E., & Gertler, F. B. (2009). Ena/VASP: towards resolving a pointed controversy at the barbed end. *Journal of Cell Science, 122*(12), 1947-1953. doi: Doi 10.1242/Jcs.038125

Chang, C., Adler, C. E., Krause, M., Clark, S. G., Gertler, F. B., Tessier-Lavigne, M., & Bargmann, C. I. (2006). MIG-10/lamellipodin and AGE-1/PI3K promote axon guidance and outgrowth in response to slit and netrin. *Curr Biol, 16*(9), 854-862. doi: 10.1016/j.cub.2006.03.083

Colo, G. P., Lafuente, E. M., & Teixido, J. (2012). The MRL proteins: adapting cell adhesion, migration and growth. *Eur J Cell Biol, 91*(11-12), 861-868. doi: 10.1016/j.ejcb.2012.03.001

Dontchev, V. D., & Letourneau, P. C. (2003). Growth cones integrate signaling from multiple guidance cues. *Journal of Histochemistry & Cytochemistry, 51*(4), 435-444.

Echarri, A., Lai, M. J., Robinson, M. R., & Pendergast, A. M. (2004). Abl interactor 1 (Abi-1) wave-binding and SNARE domains regulate its nucleocytoplasmic shuttling, lamellipodium localization, and wave-1 levels. *Mol Cell Biol, 24*(11), 4979-4993. doi: 10.1128/MCB.24.11.4979-4993.2004

Fleming, T., Chien, S. C., Vanderzalm, P. J., Dell, M., Gavin, M. K., Forrester, W. C., & Garriga, G. (2010). The role of C. elegans Ena/VASP homolog UNC-34 in neuronal polarity and motility. *Dev Biol, 344*(1), 94-106. doi: 10.1016 v/j.ydbio.2010.04.025

Hall, E. M. H. J. G. C. D. H. (1990). The unc-5, unc-6, and unc-40 genes guide circumferential migrations of pioneer axons and mesodermal cells on the epidermis in C. elegans. *Neuron, 4*(1). doi: http://dx.doi.org/10.1016/0896-6273(90)90444-K

Hannes E. Bulow, T. B., and Oliver Hobert. (2004). Differential Functions of the C. elegans FGF Receptor in Axon Outgrowth and Maintenance of Axon Position. *Neuron, 42*.

Harterink, M., Kim, D. H., Middelkoop, T. C., Doan, T. D., van Oudenaarden, A., & Korswagen, H. C. (2011). Neuroblast migration along the anteroposterior axis of C. elegans is controlled by opposing gradients of Wnts and a secreted Frizzled-related protein. *Development, 138*(14), 2915-2924. doi: 10.1242/dev.064733

Hedgecock, E. M., Culotti, J. G., Hall, D. H., Stern, B. D. (1987). Genetics of cell and axon migrations in Caenorhabditis elegans. *Development, 100*(3), 365-382.

James E. Bear, M. K., Joseph J. Loureiro, Ivan V. Maly, Gary G. Borisy, Tatyana M. Svitkina, Dorothy A. Schafer, Geraldine A. Strasser, Oleg Y. Chaga, John A. Cooper, and Frank B. Gertler. (2002). Antagonism between Ena/VASP Proteins and Actin Filament Capping Regulates Fibroblast Motility. *Cell, 109*.

Klein, R. (2004). Eph/ephrin signaling in morphogenesis, neural development and plasticity. *Curr Opin Cell Biol, 16*(5), 580-589. doi: 10.1016/j.ceb.2004.07.002

Kolodkin, A. L., & Tessier-Lavigne, M. (2011). Mechanisms and molecules of neuronal wiring: a primer. *Cold Spring Harb Perspect Biol, 3*(6). doi: 10.1101/cshperspect.a001727

Krause, M., Leslie, J. D., Stewart, M., Lafuente, E. M., Valderrama, F., Jagannathan, R., . . . Gertler, F. B. (2004). Lamellipodin, an Ena/VASP ligand, is implicated in the regulation of lamellipodial dynamics. *Dev Cell, 7*(4), 571-583. doi: 10.1016/j.devcel.2004.07.024

Li HS, C. J., Wu W, Fagaly T, Zhou L, Yuan W, Dupuis S, Jiang ZH, Nash W, Gick C, Ornitz DM, Wu JY, Rao Y. (1999). Vertebrate Slit, a Secreted Ligand for the Transmembrane Protein Roundabout, Is a Repellent for Olfactory Bulb Axons. *Cell*.

Manser, J., Roonprapunt, C., & Margolis, B. (1997). C. elegans cell migration gene mig-10 shares similarities with a family of SH2 domain proteins and acts cell nonautonomously in excretory canal development. *Dev Biol, 184*(1), 150-164. doi: 10.1006/dbio.1997.8516

Marc Tessier-Lavigne, M. P., Andrew G. S. Lumsden, Jane Dodd & Thomas M. Jessell. (1988). Chemotropic guidance of developing axons in the mammalian central nervous system. *Nature, 336*.

McShea, M. A., Schmidt, K. L., Dubuke, M. L., Baldiga, C. E., Sullender, M. E., Reis, A. L., . . . Ryder, E. F. (2013). Abelson interactor-1 (ABI-1) interacts with MRL adaptor protein MIG-10 and is required in guided cell migrations and process outgrowth in C. elegans. *Dev Biol, 373*(1), 1-13. doi: 10.1016/j.ydbio.2012.09.017

Pan, C. L., Howell, J. E., Clark, S. G., Hilliard, M., Cordes, S., Bargmann, C. I., & Garriga, G. (2006). Multiple Wnts and frizzled receptors regulate anteriorly directed cell and growth cone migrations in Caenorhabditis elegans. *Dev Cell, 10*(3), 367-377. doi: 10.1016/j.devcel.2006.02.010

Patel, F. B., Bernadskaya, Y. Y., Chen, E., Jobanputra, A., Pooladi, Z., Freeman, K. L., . . . Soto, M. C. (2008). The WAVE/SCAR complex promotes polarized cell movements and actin enrichment in epithelia during C. elegans embryogenesis. *Dev Biol, 324*(2), 297-309. doi: 10.1016/j.ydbio.2008.09.023

Quinn, C. C., Pfeil, D. S., Chen, E., Stovall, E. L., Harden, M. V., Gavin, M. K., . . . Wadsworth, W. G. (2006). UNC-6/netrin and SLT-1/slit guidance cues orient axon outgrowth mediated by MIG-10/RIAM/lamellipodin. *Curr Biol, 16*(9), 845-853. doi: 10.1016/j.cub.2006.03.025

Quinn, C. C., Pfeil, D. S., & Wadsworth, W. G. (2008). CED-10/Rac1 mediates axon guidance by regulating the asymmetric distribution of MIG-10/lamellipodin. *Curr Biol, 18*(11), 808-813. doi: 10.1016/j.cub.2008.04.050

Schmidt, K. L., Marcus-Gueret, N., Adeleye, A., Webber, J., Baillie, D., & Stringham, E. G. (2009). The cell migration molecule UNC-53/NAV2 is linked to the ARP2/3 complex by ABI-1. *Development, 136*(4), 563-574. doi: 10.1242/dev.016816

Silhankova, M., & Korswagen, H. C. (2007). Migration of neuronal cells along the anterior-posterior body axis of C. elegans: Wnts are in control. *Curr Opin Genet Dev, 17*(4), 320-325. doi: 10.1016/j.gde.2007.05.007

Spalice, A., Parisi, P., Nicita, F., Pizzardi, G., Del Balzo, F., & Iannetti, P. (2009). Neuronal migration disorders: clinical, neuroradiologic and genetics aspects. *Acta Paediatr, 98*(3), 421-433. doi: 10.1111/j.1651-2227.2008.01160.x

Stavoe, A. K., Nelson, J. C., Martinez-Velazquez, L. A., Klein, M., Samuel, A. D., & Colon-Ramos, D. A. (2012). Synaptic vesicle clustering requires a distinct MIG-10/Lamellipodin isoform and ABI-1 downstream from Netrin. *Genes Dev, 26*(19), 2206-2221. doi: 10.1101/gad.193409.112

Stiles, J., & Jernigan, T. L. (2010). The basics of brain development. *Neuropsychol Rev, 20*(4), 327-348. doi: 10.1007/s11065-010-9148-4

Valiente, M., & Marin, O. (2010). Neuronal migration mechanisms in development and disease. *Curr Opin Neurobiol, 20*(1), 68-78. doi: 10.1016/j.conb.2009.12.003

Xu, Y., & Quinn, C. C. (2012). MIG-10 functions with ABI-1 to mediate the UNC-6 and SLT-1 axon guidance signaling pathways. *PLoS Genet, 8*(11), e1003054. doi: 10.1371/journal.pgen.1003054

Yazdani, U., & Terman, J. R. (2006). The semaphorins. *Genome Biol, 7*(3), 211. doi: 10.1186/gb-2006-7-3-211

Zinovyeva, A. Y., Yamamoto, Y., Sawa, H., & Forrester, W. C. (2008). Complex network of Wnt signaling regulates neuronal migrations during Caenorhabditis elegans development. *Genetics, 179*(3), 1357-1371. doi: 10.1534/genetics.108.090290

Zou, Y. (2006). Navigating the anterior-posterior axis with Wnts. *Neuron, 49*(6), 787-789. doi: 10.1016/j.neuron.2006.03.004